Ph.D. Thesis

Expression and function of homeodomain-interacting protein kinase-2 (HIPK-2) in white and brown adipocytes

Graduate School, Keimyung University

School of Medicine

Anil Kumar Yadav

Anil Kumar Yadav

Advisor: Prof. Byeong-Churl Jang

February 2021

February 2021

Expression and function of homeodomain-interacting protein kinase-2 (HIPK-2) in white and brown adipocytes

Advisor: Prof. Byeong-Churl Jang

A Thesis Submitted for Doctoral Degree

February 2021

Graduate School, Keimyung University

School of Medicine

Anil Kumar Yadav

Anil Kumar Yadav's Ph.D. Thesis is Approved

Committee Chair: Prof. Jee-In Kim

Committee Member: Prof. Yun-Han Lee

Committee Member: Prof. Young-Sung Suh

Committee Member: Prof. Young-Chae Chang

Committee Member: Prof. Byeong-Churl Jang

Graduate School, Keimyung University

February 2021

Acknowledgment

I would like to express my sincere gratitude to my supervisor, Prof. Byeong-Churl Jang for the continuous support of my Ph.D. study and related research, for his patience, motivation, and immense knowledge. I would like to thank you for encouraging my research and for allowing me to grow as an independent researcher. Your advice and guidance on both scientific research as well as on my career have been invaluable. I have been extremely lucky to have a supervisor who cared so much about my work, and who responded to my questions and queries so promptly. I would also like to acknowledge his vigorous training for developing research competency, achieving determination for scientific research, and writing scientific articles throughout my graduate studies. Ever since Prof. Jang has supported me not only by providing a research assistantship during my Ph.D. tenure but also academically and emotionally through the rough road to finish this thesis. Also, I appreciate your efforts in creating a friendly environment within our group for easy collaboration and mutual growth.

Additionally, I would like to thank my Ph.D. committee members, which include Prof. Kim Jee In, Prof. Yun-Han Lee, Prof. Young-Sung Suh, and Prof. Young-Chae Chang for their consistent guidance, invaluable scientific advice, and constructive comments on my research work and Ph.D. thesis. I am deeply indebted to Dr. Yu-Kyoung Park for her invaluable advice and guidance on the design of various experiments and data processes. It also has been a pleasure to work with present and former members of our laboratory. Special thanks to Hyo-shin Kwon, Shailashree, Saini, and Faridul for their cooperation and friendship.

I thank Dr. Jin-ki Jung for his brotherly care and support. I am lucky to have friends or seniors in Korea; Dr. Anil Chauhan, Dr. Ashutosh, Dr. Vivek Bajpai, Dr. Mahesh, and Santosh for countless technical discussions, advice, and support.

I sincerely thank my parents and brothers for their love and care. They have always been supportive and allowed me to follow my dreams and ambitions. Finally, I want to thank my wife, Seema, who has exceptionally. supported and encouraged me throughout this journey Without her patience, intellectual and motivational support, I may never have completed this thesis work. Above all, I owe it all to Almighty God for granting me the wisdom, health, and strength to undertake this research task and enabling me to its completion.

February 2021

Anil Kumar Yadav

Contents

List of Tables

List of Figures

1. Introduction

1.1. Background of the study:

Obesity is a global pandemic that is highly responsible for the elevation of non-communicable diseases including hyperlipidemia, type 2 diabetes, cancer, and cardiovascular disease (1-2). The prevalence of obesity is a worldwide problem, with 13% of the adult population reported as being clinically obese (3). It is mainly characterized by abnormal lipid accumulation as a result of adipocyte hyperplasia (significant rise in fat cell number) and hypertrophy (in fat cell size) (4,5). A wealth of information illustrates that excessive preadipocyte differentiation causes accumulation and storage of high fat, mainly in the form of triglyceride (TG), in mature adipocytes, which resultantly leads to irregular development of the adipose tissue and thereby the burgeoning of obesity (6,7). Evidence also strongly indicates that numerous factors such as environmental and nutritional values, genetic and endocrine abnormalities are closely linked to the induction of obesity (8,9).

White adipose tissue (WAT) in the human body was earlier considered as only an energy storage organ. However, WAT is currently recognized as an endocrine organ that controls energy metabolism and homeostasis (10) by secreting not only more than 600 bioactive factors known as adipokines but also different kinds of fatty acids and metabolites (11). Among them, adipokines largely influence adipocyte differentiation, metabolism, and function (12,13).

Preadipocyte differentiation, also known as adipogenesis, is a tightly controlled process that takes place in the form of morphological biochemical, and cellular parameters (7). This process transforms fibroblast-like preadipocytes into differentiated (or mature) adipocytes filled with numerous lipid droplets (LDs) (14,15). Diverse adipogenic transcription factors, including CCAAT/enhancer-binding proteins (C/EBPs), peroxisome proliferator-activated receptors (PPARs), and signal transducer and activator of transcription (STAT) family proteins, plays a key role in preadipocyte differentiation (16-19).

Preadipocyte differentiation also involves lipogenesis and LDs maturation/stabilization, which requires fatty acid synthase (FAS), acetyl-CoA carboxylase (ACC), and perilipin A (20-23). Increasing evidence further indicates that several protein kinases, including protein kinase A (PKA), cAMP-activated protein kinase (AMPK), extracellular signal-regulated protein kinase-1/2 (ERK-1/2), p38 mitogen-activated protein kinase (MAPK), and protein kinase C (PKC), participate in the regulation of preadipocyte differentiation (21,24-27).

Lipolysis is a process in which triglyceride's ester bonds are cleaved, resulting in the generation of free fatty acids and glycerol molecules (28). Hormone-sensitive lipase (HSL) is a master regulator in the mobilization of fatty acids from stored TG and is phosphorylated (activated) by PKA, ERK-1/2, and cAMP in adipocytes (29,30). Thus, inhibition of excessive adipogenesis and/or promotion of lipolysis during preadipocyte differentiation or in mature adipocytes could be a therapeutic option against obesity.

Homeodomain-interacting protein kinase-2 (HIPK-2) is a member of the HIPKs family with serine/threonine kinase activity, which is composed of HIPK-1, HIPK-2, HIPK-3, and HIPK-4, and highly conserved in vertebrates (31). HIPK-1 to 3 were originally discovered by their ability to bind homeobox factors (31) while HIPK-4 was identified by the human genome sequence based on the high homology with the other three members (32).HIPK-2 is well characterized and regulates several transcriptional coactivators, corepressors, and kinases, which affect the expression of multiple genes that are involved, cell survival, proliferation, response to DNA damage, apoptosis, invasion, hypoxia, differentiation, and development (31, 33-36).

It has been well documented that HIPK-2 directly binds to several partners including Transformation-related protein (Trp53), C-terminal binding protein 1 (Ctbp1), MYB proto-oncogene (c-Myb), p300, High-mobility group protein HMG-I/HMG-Y (Hmga1), Zyxin, Histone H2B (H2B), Proprotein convertase 2 (Pc2), β-catenin, E3 ubiquitin-protein ligase SIAH2 (Siah2), and methyl CpG binding protein 2 (MeCP2) (37,38). Importantly, recent evidence illustrates that HIPK-2 directly interacts with CCAAT-enhancer-binding protein-β (C/EBP-β) in mouse 3T3-L1 preadipocytes, and silencing of HIPK-2 expression disrupts adipocyte differentiation of 3T3-L1 cells, addressing a physiological C/EBP-β-dependent differentiation process with functional cooperation of C/EBP-β and HIPK-2 (39).Previously, it also has been reported that HIPK-2 plays an important role in the differentiation and development of white adipocytes, and HIPK-2 knockout mice have reduced white adipose tissue mass and increased insulin sensitivity, pointing out its involvement in white adipocyte differentiation and development as well as insulin signaling in this white adipocyte (40).

While these better-understood responses exist, there is still a limited study about the role and expression regulation of HIPK-2 in white and brown adipocyte differentiation, and/or lipolysis. Besides, there is currently a limited number of commercially available HIPK-2 inhibitors.

1.2. Aims of the study:

This research was aimed to:

1. To delineate the molecular and signaling mechanisms of how HIPK-2 is up-regulated during white and brown preadipocyte differentiation.

2. To understand the function of HIPK-2 in white preadipocyte differentiation and lipolysis in mature white adipocytes.

3. To understand the function of HIPK-2 in brown preadipocyte differentiation.

4. To develop novel HIPK-2 inhibitor(s) and characterize its effects and action mechanism in white preadipocyte differentiation and lipolysis in mature white adipocytes.

5. To develop novel HIPK-2 inhibitor(s) and characterize its effects and action mechanism in brown preadipocyte differentiation.

2. Materials and methods

2.1. Drugs and chemicals:

Dulbecco's Modified Eagle's Medium (DMEM), fetal bovine serum (FBS), and penicillin/streptomycin mixture were bought from Welgene Inc. (Daegu, Republic of Korea). CX-4945 was acquired from Selleckchem (Houston, TX, USA). Control shRNA and HIPK-2 shRNA were bought from Santa Cruz Biotechnology (Delaware, CA, USA). 3-isobutyl-1-methylxanthine (IBMX), dexamethasone, and insulin were purchased from Sigma (St. Louis, MO, USA). Western Bright TM enhanced chemiluminescence (ECL) was purchased from Advansta Corporation (San Jose, CA, USA). Antibodies used in this study are mentioned in Table 1.

2.2. Cell culture:

Murine 3T3-L1 preadipocytes (CL-173™, ATCC, Manassas, VA, USA) and immortalized brown preadipocytes were grown in DMEM (high glucose) complemented by 10% heat-inactivated fetal calf serum (FCS, Gibco, Gaithersburg, MD, USA) and 1% penicillin-streptomycin cocktail at 37 ºC in a 5% CO_2 incubator.

2.3. Differentiation of 3T3-L1 and immortalized brown preadipocytes:

Both 3T3-L1 white and brown preadipocytes were cultured in DMEM containing 10% fetal calf serum and penicillin/streptomycin mixture and maintained up to the contact inhibition stage for 2 days. Differentiation of 3T3-L1 was stimulated by adding induction media containing 10% FBS along with mixtures of hormones (MDI) such as 0.5 mM IBMX (M), 0.5 μM dexamethasone (D), and 5 μg/mL insulin (I) with or without drugs (CX-4945 and KMU-011-401) at the indicated concentrations. After 48 h of MDI-induction, DMEM supplemented with 10% FBS and 5 μg/mL insulin with or without drugs (CX-4945 and KMU-011-401) at the indicated concentrations was replaced for the next 3 day. After day (D) 5, cells were nourished every day with DMEM supplemented with 10% FBS in the presence or absence of drugs (CX-4945 and KMU-011-401) until D8.

Differentiation of brown preadipocytes was stimulated by replacing media with DMEM having 10% FBS and a mixture of different stimulators such as 0.5 mM IBMX, 0.5 μM dexamethasone, 1 μg/mL insulin, 0.125 mM indomethacin (Sigma, St. Louis, MO, USA), and 1 nM T3 (Sigma, St. Louis, MO, USA) with or without CX-4945 and/or KMU-011401. After 2 days, differentiation media was changed with DMEM having 10% FBS, 1 μg/mL insulin, and 1 nM T3 with or without drugs (CX-4945 and KMU-011-401). After D5, media was replaced every day with DMEM with 10% FBS in the presence or absence of drugs (CX-4945 and KMU-011-401) until the D7.

2.5. Oil Red O staining:

On day seven or eight of differentiation conditioned brown or 3T3-L1 adipocytes were rinsed with phosphate-buffered saline (PBS) with 10% formaldehyde at room temperature (RT). Later, fixed cells were washed with 60% isopropanol and dried. A working solution of Oil Red O was layered onto the cells. After 1 h, stained cells were washed with distilled water, and stored intracellular lipid droplets were visualized using an inverted microscope (Nikon, Tokyo, Japan).

2.6. Cell survival assay:

Both 3T3-L1 or brown preadipocytes were cultivated under the above-mentioned differentiation conditions in 24-well plates. On D7 or D8 of differentiation, control or HIPK-2 inhibitors (CX-4945 and KMU-011-401, KMU-011-402, KMU-011-403, KMU-011-404, KMU-011-323) treated 3T3-L1 or brown adipocytes, which are not be stained with trypan blue dye, were counted under a microscope, respectively. The cell count assay was done in triplicates. Data are mean ± standard error (SE) of three independent experiments.

2.7. Measurement of intracellular triglyceride (TG) content:

On D7 or D8 of differentiation, intracellular TG content in control or HIPK-2 inhibitors (CX-4945 and KMU-011-401-404,323)-treated 3T3-L1 or brown adipocytes were quantified using AdipoRed reagent kit (Lonza, Basel, Switzerland), according to manufacturer's protocol, respectively. Fluorescence intensity was quantified with excitation and emission at 485 and 572 nm, respectively, using Victor3 (Perkin Elmer, CT, USA).

2.8. Quantification of glycerol content:

On D8, fat accumulated 3T3-L1 adipocytes were placed in serum-free media for 2 h and later incubated with CX-4945 (15 μM) or isoproterenol (ISO, 20 μM) for an additional 3 h and 24 h, respectively. At designated periods, the culture medium was saved, and glycerol content was quantified using free glycerol reagent (Sigma, St. Louis, MO, USA) as per the manufacturer's instructions.

2.9. Preparation of whole-cell lysates:

At the designated periods, 3T3-L1 cells were homogenized in RIPA buffer (Sigma, St. Louis, MO, USA) followed by centrifugation at

12,074 ×g for 20 min. Cell extract was collected and concentration was evaluated by bicinchoninic acid (BCA) protein assay kit (Thermo Scientific, Rockford, IL, USA).

2.10. Immunoblot analysis:

Proteins (50 μg) were subjected to SDS-polyacrylamide gel electrophoresis. Following electrophoresis, resolved proteins were transferred onto polyvinylidene difluoride membrane (PVDF, Millipore, Bedford, MA, USA) by electroplating. Membranes blocked with 5% skim milk prepared in TBST (1×) and subsequently incubated with specific antibodies listed in Table 1 at 4 ℃. After overnight incubation, membranes were washed three times with TBST (1×) followed by horseradish peroxidase-conjugated secondary antibodies for 2 h at RT. Next, immunoblots were rinsed three times with TBST (1×) and protein-antibody complexes were visualized using enhanced chemiluminescence (ECL) reagents (Advansta, CA, USA). Actin and total S6 proteins were used as an equal protein loading control.

2.11. Quantitative real-time RT-PCR:

Total RNA was obtained from control or HIPK-2 inhibitors (CX-4945 and KMU-011-401)-treated 3T3-L1 cells using RNAiso Plus (TaKaRa, Kusatsu, Shiga, Japan). The isolated RNA (3 μg) was converted to cDNA using a random hexadeoxynucleotide primer and reverse transcriptase.

SYBR green (TaKaRa, Kusatsu, Shiga, Japan) was employed to quantitatively determine transcript levels of genes with LightCyclerâ96 Machine (Roche, Mannheim, Germany). PCR reactions were run in triplicate for each sample, and transcript levels of each gene were normalized to the level of 18S rRNA. Primer sequences used in this study are listed in Table 2.

2.12. Quantification of intracellular ATP levels:

Intracellular ATP level during differentiation of 3T3-L1 preadipocytes in the presence or absence of CX-4945 or 2-deoxyglucose (2-DG) were measured with ATPLite-1step kit from PerkinElmer (CT, USA) according to the manufacturer's instructions.

2.13. Stable transfection of HIPK-2 short-hairpin RNA (shRNA):

3T3-L1 preadipocytes were transfected with control or HIPK-2 shRNA (1 μg) using Lipofectamine ™ 2000(Invitrogen, USA) according to the manufacturer's instructions. Later, stably transfected cells were selected by 1 μg/mL puromycin. Control or HIPK-2 shRNA-transfected 3T3-L1 cells were differentiated as above indicated differentiation conditions.

2.14. Statistical analysis:

All data are expressed as mean ± standard error (SE) of at least three independent experiments. Statistical significance between different groups was evaluated by one-way ANOVA followed by Dunnett's post hoc test using SPSS 11.5 software (SPSS, Inc). $P<0.05$ was considered to indicate statistical significance.

Table 1. Antibodies used for immunoblot analysis.

Antibodies	Dilution used	Source	Catalog no.
Primary antibodies			
HIPK-2	1:500	Santa Cruz Biotechnology	Sc-100383
C/EBP-α	1:2,000	Santa Cruz Biotechnology	sc-61
PPAR-γ	1:2,000	Santa Cruz Biotechnology	sc-7272
p-STAT-3 (Y705)	1:2,000	Santa Cruz Biotechnology	sc-8059
STAT-3	1:2,000	Santa Cruz Biotechnology	sc-8019
p-PKA	1:2,000	Santa Cruz Biotechnology	sc-32968
PKA	1:2,000	Santa Cruz Biotechnology	sc-98951
Perilipin A	1:2,000	BioVision	#3948-200
FAS	1:2,000	BD Bioscience	#9452
S6	1:2,000	Cell signalling	#2217
p-AMPK (T172)	1:2,000	Cell signalling	#2535
AMPK	1:2,000	Cell signalling	#2793
p-ACC (S79)	1:2,000	Cell signalling	#3661
ACC	1:2,000	Cell signalling	#3662
p-LKB-1(S334)	1:2,000	Cell signalling	#3482
LKB-1	1:2,000	Cell signalling	#3037
p-HSL (S563)	1:2,000	Cell signalling	#4139
p-HSL (S660)	1:2,000	Cell signalling	#4126
p-ERK-1/2	1:2,000	Cell signalling	#9101
ERK-1/2	1:2,000	Cell signalling	#9102
HSL	1:2,000	Cayman chemical	#10006371
β-Actin	1:10,000	Sigma	A5441
Secondary antibodies			

Goat anti-rabbit IgG-HRP	1:5,000	Jackson ImmunoResearch Laboratories	111-035-045
Goat anti-mouse-IgG-HRP	1:5,000	Jackson ImmunoResearch Laboratories	115-035-062

Table 2. Sequences of primers used for real-time PCR analysis.

Gene	Forward	Reverse
HIPK-1	TAAACGACCTCGGAGACTGC	GAGGGCTGAGATCACTGCAT
HIPK-2	CACAGGCTCAAGATGGCAGA	CCATACCTTCGTACACGGGG
HIPK-3	ATCGAAGCAGAACTGCACCA	CCAAAAGTGCCACGACCAAG
C/EBP-α	TTACAACAGGCCAGGTTTCC	GGCTGGCGACATACAGTACA
PPAR-γ	AGGCCGAGAAGGAGAAGCTGTTG	TGGCCACCTCTTTGCTCTGCTC
FAS	TTGCTGGCACTACAGAATGC	AACAGCCTCAGAGCGACAAT
Perilipin A	CTTTCTCGACACACCATGGAAAC	CCACGTTATCCGTAACACCCTTCA
Adiponectin	ACGACACCAAAAGGGCTCAG	CGTCATCTTCGGCATGACTG
Leptin	GACCGGGAAAGAGTGACAGG	AGAGCAATCTGACACCAGCC
Resistin	TGTAAGCTGCAGGTCGCTTC	CTCTGGAGCTACAGGAACGG
18S rRNA	GGTGAAGGTCGGTGTGAACG	GGTAGGAACACGGAAGGCCA

3. Results

3.1. HIPK-2 expression is highly elevated during 3T3-L1 preadipocyte differentiation:

The experimental protocol for 3T3-L1 preadipocytes differentiation is depicted in Figure 1A. Intracellular lipid accumulation during the differentiation of 3T3-L1 preadipocyte was primarily investigated using Oil Red O staining. On the day (D) 8 of differentiation, there was a high accumulation of intracellular lipid droplets (LDs) in 3T3-L1 cells, compared with undifferentiated cells on D0 (Figure 1B, upper panels). Light microscopic images also confirmed the storage of lipid droplets in 3T3-L1 cells on D8 of differentiation (Figure 1B, lower panels). Next, the protein expression levels of HIPK-2 during 3T3-L1 preadipocyte differentiation were measured using Western blot analysis. As shown in Figure 1C, there was a time-dependent elevation of HIPK-2 protein expression during 3T3-L1 preadipocyte differentiation, compared with that on D0. Triplicate experiment also confirmed the significant induction of HIPK-2 protein expression in 3T3-L1 cells on D8 of differentiation, compared with that on D0 (Figure 1D). Densitometry results of Figure 1D are depicted in Figure 1E. Next, the mRNA levels of HIPK-1, 2, and 3 were analyzed during the process of 3T3-L1 differentiation using real-time qPCR. As shown in Figure 1F, HIPK-2 mRNA expression was significantly increased on D2, D5, and D8 of 3T3-L1 preadipocyte differentiation, compared with that on D0. However, mRNA level of HIPK-1 was not significantly up-

regulated on all the times tested but HIPK-3 mRNA expression was elevated significantly D8 of 3T3-L1 preadipocyte differentiation, compared with them on D0.

3.2. p38 MAPK, JNK-1/2, PKB, and PKC are crucial for the up-regulation of HIPK-2 expression during 3T3-L1 preadipocyte differentiation:

To understand signaling mechanism(s) or factor(s) responsible for the induction of HIPK-2 mRNA expression during 3T3-L1 preadipocyte differentiation, 3T3-L1 preadipocytes were induced to differentiate in the absence or presence of PD98059 (a MEK-1/2 (ERK-1/2) inhibitor), SB203580 (a p38 MAPK inhibitor), SP600125 (a JNK-1/2 inhibitor), LY294002 (a PI3K/PKB inhibitor), vitamin E (an antioxidant) or GF109203X (a PKC inhibitor) for 5 days. As shown in Figure 2A, notably, treatment with either SB203580, SP600125, LY294002, and GF109203X greatly suppressed the up-regulation of HIPK-2 expression in 3T3-L1 cells on D5 of differentiation. However, treatment with PD98059 or vitamin E did not influence the up-regulation of HIPK-2 expression on D5 of 3T3-L1 preadipocyte differentiation. As depicted in Figure 2B, treatment with SB203580, SP600125, LY294002, and GF109203X strongly blocked the storage of fat in 3T3-L1 cells on D5 of differentiation.

3.3. Knock-down of HIPK-2 leads to less lipid accumulation and TG content during 3T3-L1 preadipocyte differentiation:

To directly confirm the biological role of HIPK-2 up-regulation in the process of 3T3-L1 preadipocyte maturation, 3T3-L1 preadipocytes that were stably transfected with short hairpin RNA (shRNA) of control or HIPK-2 were generated. As exhibited in Figure 3A and B, compared with control shRNA-transfected 3T3-L1 cells, there was a much lower expression of HIPK-2 at the mRNA expression on D2 or D5 and protein levels at D5 or D8 in HIPK-2 shRNA-transfected cells of differentiation, pointing out the HIPK-2 shRNA transfection efficiency. As shown in Figure 3C (upper panels), there was no lipid accumulation in both control and HIPK-2 shRNA-transfected 3T3-L1 cells on D0. Notably, the knock-down of HIPK-2 led to a strong suppression of fat storage compared to control on D8 of differentiation (Figure. 3C, upper panels). Light microscopy further demonstrated much less lipid accumulation in HIPK-2 shRNA-transfected 3T3-L1 cells compared with control on D8 of differentiation (Figure. 3C, lower panels).

Moreover, there was less TG content in HIPK-2 shRNA-transfected 3T3-L1 cells compared with control on D8 of differentiation, (Figure 3D). Cell count analysis was next performed to see whether the gene silencing of HIPK-2 influences the growth of 3T3-L1 cells. Evidently, there was no difference in cell survival between control and HIPK-2 shRNA-transfected 3T3-L1 cells on D8 of differentiation, illustrating knock-down of HIPK-2 did not affect these cell growth (Figure 3E).

3.4. Knock-down of HIPK-2 leads to the reduced expression and phosphorylation levels of C/EBP-α, PPAR-γ, and STAT-3 during 3T3-L1 preadipocyte differentiation:

To further elucidate the molecular mechanisms by which knock-down of HIPK-2 leads to less fat storage and TG content in the process of 3T3-L1 preadipocyte differentiation, the expression as well as activity (phosphorylation) of key adipogenic transcription factors, such as C/EBPs, PPARs, and STATs, were measured from control or HIPK-2 shRNA-transfected 3T3-L1 cells on D2, D5, and D8 of differentiation. As shown in Figure 4A, there was a decreased expression of C/EBP-α with high molecular weight (MW) on D2 and with low MW on D5 and D8 in HIPK-2 shRNA-transfected 3T3-L1 cells, compared with control shRNA-transfected cells. There was also a decreased phosphorylation of STAT-3 on D5 and D8 in HIPK-2 shRNA-transfected 3T3-L1 cells, compared with control shRNA-transfected cells. Total protein expressions of S6 and STAT-3, which was used as a loading control, was not changed. Results of real-time qPCR analyses, as shown in Figure 4B, further demonstrated the reduced mRNA expression of C/EBP-α and PPAR-γ in HIPK-2 shRNA-transfected 3T3-L1 cells, compared with control.

3.5. Knock-down of HIPK-2 leads to the reduced expression of FAS and perilipin A during 3T3-L1 preadipocyte differentiation:

Next, the expression of FAS, an enzyme responsible for fatty acid synthesis (20), and perilipin A, a LD-binding and stabilizing protein (22), was determined from control or HIPK-2 shRNA-transfected 3T3-L1 cells on D2, D5, and D8 of differentiation. As shown in Figure 5A, there was a decreased expression of FAS and perilipin A on D5 and D8 in HIPK-2 shRNA-transfected 3T3-L1 cells, compared with control shRNA-transfected cells. Total protein expression of S6 was not changed. Data of real-time qPCR analyses, as shown in Figure 5B, also showed the reduced mRNA expression of FAS and perilipin A in HIPK-2 shRNA-transfected 3T3-L1 cells, compared with control shRNA-transfected cells.

3.6. Knock-down of HIPK-2 causes the reduced expression of adiponectin, leptin, and resistin during 3T3-L1 preadipocyte differentiation:

Next, the effect of HIPK-2 knock-down on the expression of adipokines, such as adiponectin, leptin, and resistin, which are responsible for the pathogenesis of obesity and type 2 diabetes (11-13], was measured during 3T3-L1 preadipocyte differentiation. Notably, depicted in Figure 6A-C, there was a decreased mRNA expression of adiponectin and leptin on D5 and D8 in HIPK-2 shRNA-transfected 3T3-L1 cells, compared

with control shRNA-transfected cells. Also, there was a reduced mRNA expression of resisitin on D2, D5, and D8 in HIPK-2 shRNA-transfected 3T3-L1 cells, compared with control.

3.7. CX-4945, an inhibitor of HIPK-2, strongly inhibits lipid accumulation and reduces TG content during 3T3-L1 preadipocyte differentiation:

Of note, it has been recently demonstrated that CX-4945 strongly makes several interactions with the residues in the ATP-pocket of HIPK-2 and blocks its catalytic activity (41), suggesting CX-4945 as an inhibitor of HIPK-2. Next, using CX-4945, investigated its effects on fat storage and TG content during 3T3-L1 preadipocyte differentiation. As shown in Figure 7A (upper panels), compared with the mock-treated 3T3-L1 cells, CX-4945 strongly inhibited lipid accumulation in a concentration-dependent manner in 3T3-L1 cells on D8 of differentiation. Evidently, CX-4945 at 15 and 20 μM caused the maximal suppression of lipid accumulation. Furthermore, light microscopy observations also confirmed the CX-4945's lipid-decreasing effect (Figure 7A, lower panels). As further shown in Figure 7B, CX-4945 also markedly reduced TG content in a dose-dependent manner in 3T3-L1 cells on D8 of differentiation. Apparently, CX-4945 at 15 and 20 μM caused the maximal reduction of TG content. Of note, results of cell count analysis demonstrated that CX-4945 at the dosages implemented was not toxic to 3T3-L1 cells at the time tested; rather, CX-4945 at 20 μM significantly ($p<0.0105$) enhanced

the cell survival compare to control and there was no significant difference ($p<0.8589$) in cell survival at 15 μM compare to 20 μM (Figure 7C). Because of maximal suppressive impacts on lipid accumulation and TG content without any cytotoxicity, 15 μM of the CX-4945 was selected for further studies.

3.8. CX-4945 decreases expression of C/EBP-α and PPAR-γ during 3T3-L1 preadipocyte differentiation:

To delineate the underlying mechanisms by which CX4945-mediated less lipid accumulation and TG content during 3T3-L1 preadipocyte differentiation, we examined whether CX-4945 (15 μM) affects the expression/activity (phosphorylation) of key adipogenic molecules, such as C/EBPs, PPARs, on D2, D5, and D8 of differentiation. As shown in Figure 8A, there was a decreased expression of C/EBP-α with high molecular weight (MW) on D2 or D8 and with low MW on D5 and D8 in CX4945-treated 3T3-L1 cells, compared with vehicle control (DMSO; 0.1%). Furthermore, CX-4945 strongly blocked expressions PPAR-γ on D2, D5, and D8. Expression of total S6, which was used as a loading control, was consistent. Results of real-time qPCR analyses, as shown in Figure 8B, further demonstrated the reduced mRNA expression of C/EBP-α and PPAR-γ in CX-4945 treated 3T3-L1 cells, compared with vehicle control cells. Triplicate experiments also affirmed the capability of CX-4945 to impede the expressions of C/EBP-α and PPAR-γ on D8 (Figure 8C). Densitometry results of Figure 8C were exhibited in Figure 8D. Expression of total S6, which was used as a loading control, was consistent.

3.9. CX-4945 reduces expression of FAS and perilipin A during 3T3-L1 preadipocyte differentiation:

Next, we explored the effect of CX-4945 on expressions of FAS, an enzyme responsible for fatty acid synthesis (20), and perilipin A, a LD-binding and stabilizing protein (22) on D2, D5, and D8 of differentiation. As shown in Figure 9A, CX-4945 (15 μM) greatly suppressed the expression of FAS and perilipin A on D5 and D8 of 3T3-L1 differentiation compared to vehicle control cells. Expression of total S6, which was used as a loading control, was consistent. Moreover, real-time qPCR analysis data, as shown in Figure 9B, exhibited the reduced mRNA expression of perilipin A in CX-4945 treated 3T3-L1 cells on D2, D5, and D8 of differentiation, however, mRNA expressions of FAS was unchanged or slightly increased during the differentiation of 3T3-L1 preadipocytes. Triplicate experiments also affirmed the capability of CX-4945 to impede the expressions of FAS and perilipin A on D8 (Figure 9C). Densitometry results of Figure 9C were exhibited in Figure 9D. Expression of total S6, which was used as a loading control, was consistent.

3.10. CX-4945 down-regulates expression of leptin, adiponectin, and resistin during 3T3-L1 preadipocyte differentiation:

Next, Adipocytokines including adiponectin, leptin, and resistin are mainly secreted from adipose tissue. Recent studies have indicated the important aspect of adipokines in obesity and other related diseases (11-13). Herein, determined the expressions of adiponectin, leptin, and resistin after the treatment with CX-4945 (15 μM) during 3T3-L1 preadipocytes differentiation. Crucially, as exhibited in Figure 10A-C, CX-4945 strongly decreased the mRNA expressions of adiponectin, leptin, and resistin on D5 and D8 of 3T3-L1 preadipocytes differentiation compared with vehicle control.

3.11. CX-4945 increases phosphorylation of AMPK, LKB-1, and ACC during 3T3-L1 preadipocyte differentiation:

AMPK is a key controller of energy metabolism, and its activation (phosphorylation) leads to inhibition of adipogenesis (42). Therefore, we investigated whether treatment of CX-4945 could modulate AMPK phosphorylation in differentiating 3T3-L1 cells. Notably, exhibited in Figure 11A, CX-4945 (15 μM) strongly induced phosphorylation (activation) of AMPK compare to vehicle control on D5 and D8 of 3T3-L1 differentiation. Total AMPK expressions were not affected by CX-4945. ACC is a well-known subsequent molecule of AMPK and it is responsible for the synthesis of fatty acids (43). Herein, treatment with CX-4945, highly induced the phosphorylation (inactivation) of ACC on D5 and D8 of 3T3-L1 preadipocyte differentiation. Total ACC expressions were also induced by CX-4945 on D5 and D8 of treatment during 3T3-L1 differentiation. Considering that liver kinase B-1 (LKB-1) is a crucial kinase to induce phosphorylation of AMPK (44), further

determined whether LKB-1 protein is expressed and activated (phosphorylated) in differentiating 3T3-L1 cells and is regulated by CX-4945. In control cells, on D2, there were much-elevated levels of phosphorylated LKB-1, however, on days 5 and 8 of differentiating 3T3-L1 cells, its expression was strongly declined. Markedly, at D2 and D8 of differentiation, LKB-1 phosphorylation was strongly induced in CX-4945-treated cells, compared with the control. Total expression levels of LKB-1 was not affected by CX-4945 on all tested times of differentiation. Expression of total S6, which was used as a loading control, was consistent. As exhibited in Figure 11B, triplicate experiments also affirmed the capability of CX-4945 to induce phosphorylation of AMPK, ACC, and LKB-1 on D8. Expression of total S6, which was used as a loading control, was consistent. The densitometry results of Figure 11B are exhibited in Figure 11C.

3.12. CX-4945 decreases intracellular ATP content during 3T3-L1 preadipocyte differentiation:

Phosphorylation (activation) of AMPK is affected by variations in the intracellular AMP/ATP ratio (45). Therefore, next, we determined in case CX-4945 could affect intracellular ATP levels during 3T3-L preadipocytes differentiation. As depicted in Figure 12A-C, treatment of CX-4945 (15 μM) significantly reduced cellular ATP content compared to vehicle control on D5 and D8 of 3T3-L1 cells differentiation. Similarly, 2-deoxyglucose (2-DG) as a positive control, lowered cellular ATP contents on D2, D5, and D8 of adipocyte differentiation.

3.13. CX-4945 increases glycerol release and phosphorylation of HSL, ERK1/2, and perilipin A in differentiated 3T3-L1 adipocytes:

Next, we determined the effect of CX-4945 on lipolysis in differentiated 3T3-L1 adipocytes. Herein, the lipolytic effect of CX-4945 was evaluated by glycerol contents in the culture medium from the conditioned cells. As a positive control, Isoproterenol (ISO) was used (46). The experimental scheme and timescale for measurement of glycerol content and hormone-sensitive lipase (HSL) phosphorylation are depicted in Figure 13A. As shown in Figure 13B, ISO largely stimulated glycerol release at 3 and 24 h of treatment while CX-4945 also strongly stimulated glycerol release at 3 h which was further enhanced at 24 h of treatment compared to the positive control in differentiated 3T3-L1 adipocytes. Furthermore, ISO greatly enhanced the HSL phosphorylation at S563 and S660 (Figure 13C). CX-4945 greatly increased HSL phosphorylation on S563 and S660. Total HSL and actin expressions remained consistent. It has been well documented that activation of ERK1/2, perilipin A, and protein kinase A (PKA) regulates the process of lipolysis (47-50). As depicted in Figure 13D, CX-4945 induced phosphorylation (activation) of ERK1/2 at 3 and 24 h of treatment in differentiated 3T3-L1 cells. Interestingly, CX-4945-induced an electrophoretic shift (hyperphosphorylation) of expression of perilipin A. Phosphorylation or expression of PKA was not changed by the treatment with ISO or CX-4945 at 3 or 24 h in differentiated 3T3-L1 cells. Total ERK-1/2 and actin, as a loading control, remained consistent.

3.14. PD98059 greatly blocks the CX-4945-induced lipolysis, glycerol release, and phosphorylation of HSL, ERK1/2, and perilipin A in differentiated 3T3-L1 adipocytes:

In order to evaluate the potential role of the ERK1/2 activation in lipolysis, PD98059, a specific MEK1/2 inhibitor, was used to inhibit activation of the MEK signaling. As shown in Figure 14A, CX-4945 or ISO strongly stimulated the release of glycerol indifferentiated 3T3-L1 cells. Notably, combined incubation of PD98059 significantly blocked the glycerol releasing effects of CX-4945 and ISO in differentiated 3T3-L1 cells. As exhibited in Figure 14B, at mechanistic levels, treatment of PD98059 strongly reduced the basal as well as CX-4945-induced ERK-1/2 phosphorylation without changing total ERK protein expression (Figure 14C). Furthermore, PD98059 downregulated the CX4945-induced phosphorylation of HSL at S563 and reversed electrophoretic shift (hyperactivation) of perilipin A expressions in differentiated 3T3-L1 cells. Total HSL and actin expressions were consistent.

3.15. KMU-011401, a novel HIPK-2 inhibitor, strongly blocks lipid accumulation and TG content during 3T3-L1 preadipocyte differentiation:

Due to the very limited commercial availability of HIPK-2 inhibitors, a series of novel HIPK-2 inhibitors (KMU-011401, KMU-011402, KMU-

011403, KMU-011404, and KMU-011323) were synthesized by medicinal chemistry and tested for their suppressive effects at a final concentration of 10 μM on lipid storage and TG content during 3T3-L1 preadipocyte differentiation. As depicted in Figure 15A (upper panels), KMU-011401, KMU-011402, KMU-011403, KMU-011404, and KMU-011323 greatly blocked fat storage during 3T3-L1 preadipocyte differentiation. Light microscopic images also confirmed the lipid-lowering effects of each of these chemicals (Figure 15A, lower panels). However, light microscopic images showed that KMU-011403 at 10 μM was cytotoxic to 3T3-L1 cells on D8. In fact, KMU-011403-induced cytotoxicity was easily visible even on D2 of differentiation (data not shown). Further, results of AdipoRed assay revealed that KMU-011401, KMU-011402, KMU-011403, KMU-011404, and KMU-011323 significantly reduced TG content in 3T3-L1 cells on D8 of differentiation (Figure 15B). Data of cell count analysis demonstrated that KMU-011401, KMU-011402, KMU-011404, and KMU-011323 did not change the growth of 3T3-L1 cells on D8 of differentiation, whereas KMU-011403 significantly reduced the number of cells survived (Figure 15C). These results point out that KMU-011403's lipid-reducing effect seen herein was related to its cytotoxicity.

Overall, based on the facts that KMU-011401 at 10 μM strongly blocked lipid accumulation and decreased TG content with no cytotoxicity (along with most healthy cell morphology) during adipocyte differentiation, KMU-011401 was selected for further studies. The concentration-dependent effects of KMU-011401 on lipid accumulation and TG content during 3T3-L1 preadipocyte differentiation was next investigated. As shown in Figure 15D (upper panels), compared with the mock-treated 3T3-L1 cells, KMU-011401 strongly inhibited lipid

accumulation in a dose-dependent manner in 3T3-L1 cells on D8 of differentiation. Apparently, KMU-011401 at 1 to 10 μM caused the strong inhibition of lipid accumulation. The KMU-011401's lipid-reducing effects were also confirmed by light microscopy (Figure 15D, lower panels). As also shown in Figure 15E, KMU-011401 markedly reduced TG content in a concentration-dependent manner in 3T3-L1 cells on D8 of differentiation. Similarly, KMU-011401 at 5 or 10 μM caused the maximal reduction of TG content. Of interest, results of cell count analysis showed that KMU-011401 at the doses applied was not cytotoxic to 3T3-L1 cells at the time tested (Figure 15F). CX-4945 (15 μM) was used for comparative results. Because of maximal suppressive effects on lipid accumulation and TG content with no cytotoxicity, the concentration of 5 μM of KMU-011401 was selected for further studies.

3.16. HIPK-2 expression is significantly increased during brown preadipocyte differentiation:

The experimental protocol for the differentiation of brown preadipocytes into adipocytes is depicted in Figure 16A. Intracellular lipid accumulation during brown preadipocyte differentiation was initially determined by Oil Red O staining. Comparative to undifferentiated brown preadipocytes, there was high lipid accumulation in brown adipocytes on D7 of differentiation (Figure 16B, upper panels). Light microscopic images also demonstrated an increased lipid accumulation in brown adipocytes on D7 of differentiation

(Figure 16B, lower panels). Next, the mRNA expression of HIPK-2 during the differentiation of brown preadipocytes into adipocytes was determined using real-time qPCR. As shown in Figure 16C, there was a time-dependent increase in HIPK-2 mRNA expression during brown preadipocyte differentiation.

3.17. p38 MAPK and PKC are crucial for the induction of HIPK-2 expression during brown preadipocytes differentiation:

In a way to understand molecular signaling mechanism(s) or factor(s) culpable for the elevation of expressions of HIPK-2 during differentiation of brown preadipocyte, we executed a pharmacological inhibition study using SB203580 (a p38 MAPK inhibitor), PD98059 (a MEK-1/2 (ERK-1/2) inhibitor), SP600125 (a JNK-1/2 inhibitor), LY294002 (a PI3K/PKB inhibitor), vitamin E (an antioxidant) or GF109203X (a PKC inhibitor). Strikingly, as depicted in Figure 17A, treatment with either SB203580, LY294002, and GF109203X strongly repressed the elevation of HIPK-2 expression on D7 of brown preadipocyte differentiation, without cytotoxicity (Figure 18A). However, although treatment with SP600125 strongly suppressed the induction of HIPK-2 expression on D7 of brown preadipocyte differentiation, the drug was highly cytotoxic to these cells. As shown in Figure 17B, treatment with either SB203580, LY294002, or GF109203X strongly blocked the lipid accumulations on D7 of in brown preadipocyte differentiation.

3.18. CX-4945 potently repressed lipid accretion and triglyceride (TG) synthesis during brown preadipocytes differentiation:

Next, we examined that the pharmacological inhibition of HIPK-2 using CX-4945 affects lipid accumulation and TG content during brown preadipocyte differentiation. As depicted in Figure 18A (upper panels), compared with the mock-treated brown cells, CX-4945 firmly decreased lipid accumulation in a concentration-dependent manner on D7 of differentiation. Notably, CX-4945 at 5, 10, 15, and 20 μM caused the maximal suppression of lipid accumulation. The CX-4945's lipid-reducing effect was also confirmed by light microscopy (Figure 18A, lower panels). As further shown in Figure 18B, CX-4945 also markedly reduced TG content in a dose-dependent manner in brown cells on D7 of differentiation. Of note, results of cell count analysis demonstrated that CX-4945 up to 15 μM was not cytotoxic to brown cells, however, CX-4945 at 20 μM significantly reduced the cell survival (Figure 18C).

3.19. KMU-011401 dose-dependently decreased lipid accumulation and triglyceride (TG) content during brown preadipocytes differentiation:

Next, examined the effect of KMU-011401, a novel HIPK-2 inhibitor on lipid accumulation and TG content during brown preadipocyte differentiation. As shown in Figure 19A (upper panels), KMU-011401

strongly reduced lipid accumulation in a concentration-dependent manner on D7 of differentiation. Notably, KMU-011401 at 5 and 10 μM greatly caused the maximal suppression of lipid accumulation. The KMU-011401's lipid-reducing effect was also confirmed by light microscopy (Figure 19A, lower panels). As further shown in Figure 19B, KMU-011401 firmly reduced TG content in a dose-dependent manner in brown cells on D7 of differentiation. Of note, results of cell count analysis demonstrated that KMU-011401 at the doses applied was not cytotoxic at D7 of brown cell differentiation (Figure 19C).

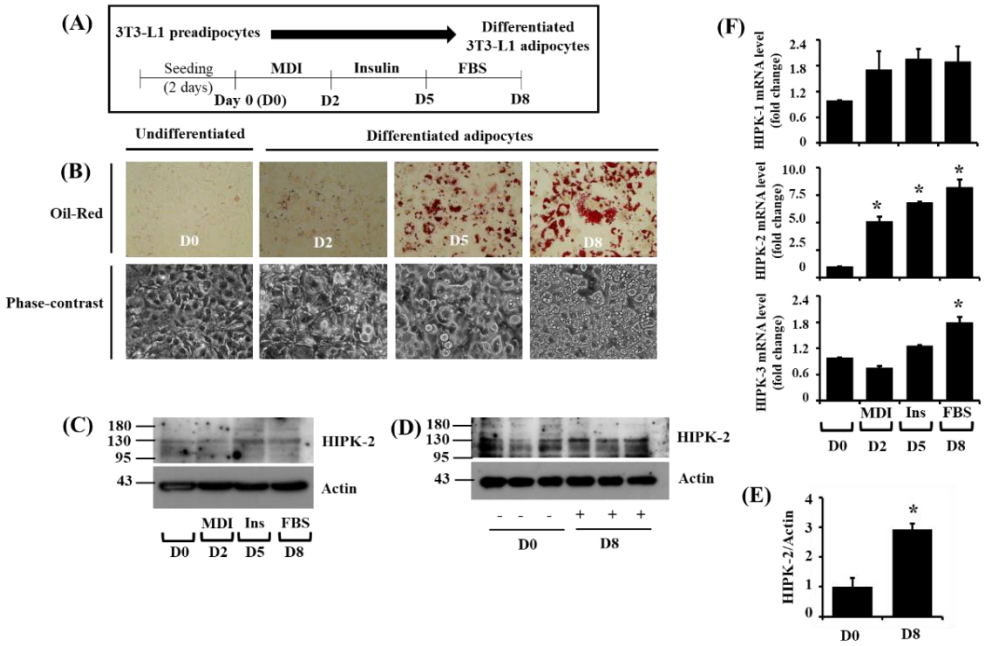

Figure 1. Lipid accumulation and expression of HIPK-2 during 3T3-L1 preadipocyte differentiation. (A) Experimental scheme of 3T3-L1 preadipocyte differentiation. (B) Determination of lipid droplets (LDs) accumulation on day 0 (D0), D2, D5, and D8 of 3T3-L1 preadipocyte differentiation by Oil Red O staining (upper panels) and by phase-contrast image (lower panels). (C) 3T3-L1 preadipocytes were differentiated with induction medium and harvested at D0, D2, D5, and D8, respectively. At each time point, whole-cell lysates were prepared and analyzed by immunoblot analysis with respective antibodies. (D,E) Western blot analysis in triplicate experiments on D8 (D) and the densitometry data of D (E). (F) Total cellular RNA was extracted and analyzed by real-time qPCR with respective

primers. Data are mean ± SE (n=3). $^{*}p < 0.05$ compared to the value of vehicle control.

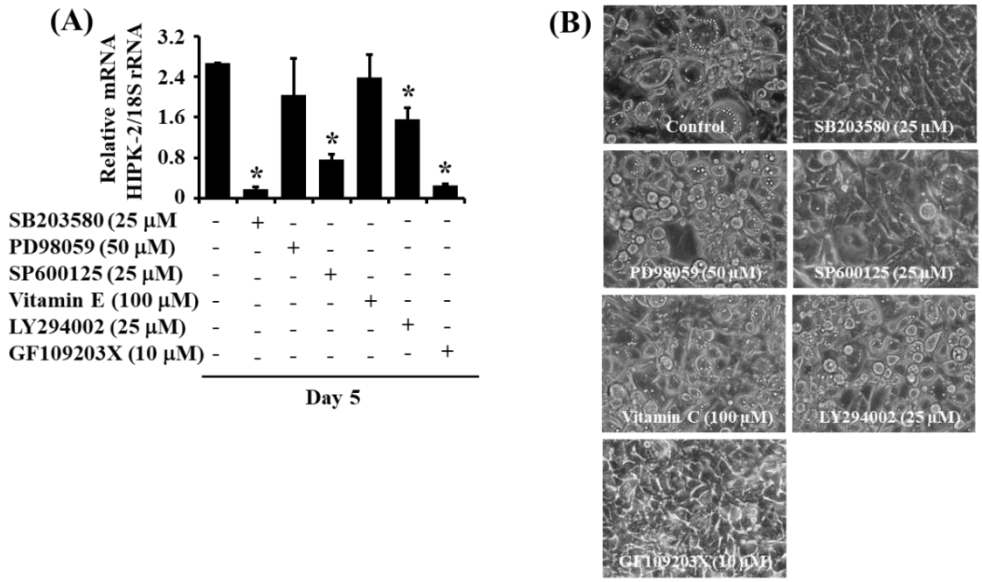

Figure 2. Effects of SB203580, PD98059, SP600125, LY294002, vitamin E or GF109203X on the expression of HIPK-2 on D5 of 3T3-L1 preadipocyte differentiation. (A,B) 3T3-L1 preadipocytes were differentiated with induction medium in the absence (control; 0.1 % DMSO) or presence of SB203580 (a p38 MAPK inhibitor), PD98059 (a MEK-1/2 (ERK-1/2) inhibitor), SP600125 (a JNK-1/2 inhibitor), LY294002 (a PI3K/PKB inhibitor), vitamin E (an antioxidant) or GF109203X (a PKC inhibitor) at designated concentrations, and harvested at day 5 (D5). Total cellular RNA was then extracted and analyzed by real-time qPCR with respective primers (A) and cellular lipid contents were assessed phase-contrast images after the treatment (B). Data are mean ± SE (n=3). *$p<0.05$ compared to the value of vehicle control.

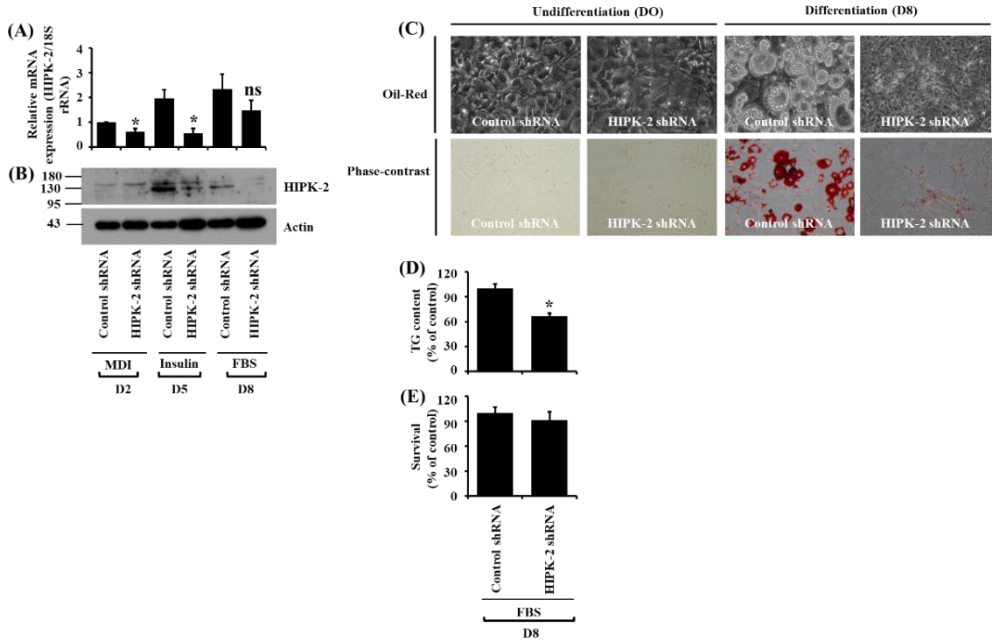

Figure 3. Effects of gene silencing of HIPK-2 on expression of HIPK-2, lipid accumulation, TG content, and cell survival during 3T3-L1 preadipocyte differentiation. (A,B) 3T3-L1 preadipocytes were stably transfected with 1 μg of control or HIPK-2 shRNA. Conditioned cells were differentiated with an induction medium containing MDI, insulin, and FBS, and harvested at day 0 (D0), D2, D5, and D8, respectively. At each time point, total cellular RNA and protein were extracted and analyzed by real-time qPCR (A) or Western blotting (B), respectively. Data are mean ± SE (n=3) of three independent experiments. *p<0.05 vs. control at respective day. (C,D,E) After-above mentioned conditions, lipid droplets accumulation in control or HIPK-2 shRNA-transfected cells on D8 was measured by Oil Red O staining (upper panels) and by phase-contrast image (lower panels)

(C), cellular TG content by AdipoRed assay (D) or cell survival (E) by cell count analysis on D8 of adipocyte differentiation. Data are mean ± SE (n=3). *p<0.05 vs. control (D8).

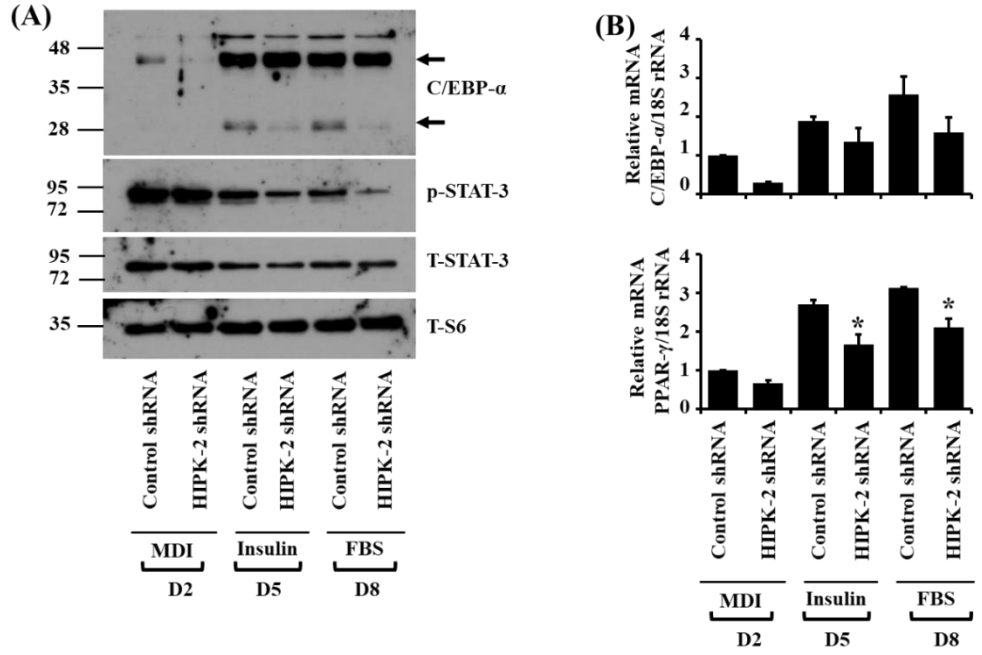

Figure 4. Effects of gene silencing of HIPK-2 on expression and/or phosphorylation of C/EBP-α, PPAR-γ, and STAT-3 during 3T3-L1 preadipocyte differentiation. (A) 3T3-L1 preadipocytes were stably transfected with 1 μg of control or HIPK-2 shRNA. Control or HIPK-2 shRNA-transfected cells were differentiated with an induction medium containing MDI, insulin, and FBS, and harvested at day 0 (D0), D2, D5, and D8, respectively. At each time point, whole-cell lysates were prepared and analyzed by immunoblot analysis with respective antibodies. (B) After the above-mentioned conditions, at each time point, total cellular RNA was prepared and analyzed by real-time qPCR with respective primers. Data are mean ± SE (n=3). *$p<0.05$ vs. control at respective day.

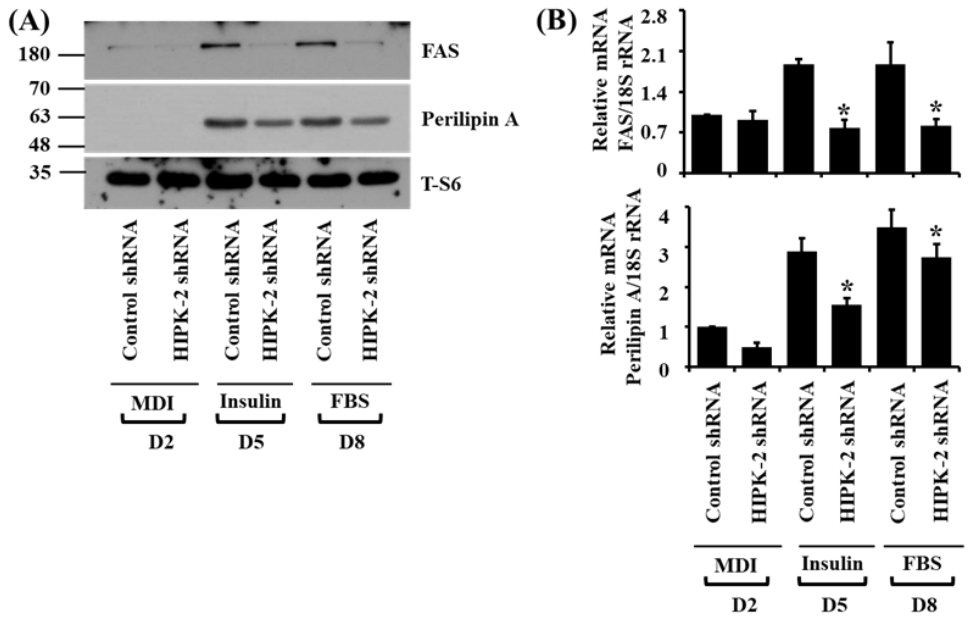

Figure 5. Effects of gene silencing of HIPK-2 on expression of FAS and perilipin A during 3T3-L1 preadipocyte differentiation. (A) 3T3-L1 preadipocytes were stably transfected with 1 μg of control or HIPK-2 shRNA. Control or HIPK-2 shRNA-transfected cells were differentiated with an induction medium containing MDI, insulin, and FBS, and harvested at day 0 (D0), D2, D5, and D8, respectively. At each time point, whole-cell lysates were prepared and analyzed by immunoblot analysis with respective antibodies. (B) After the above-mentioned conditions, at each time point, total cellular RNA was prepared and analyzed by real-time qPCR with respective primers. Data are mean ± SE (n=3). *$p<0.05$ vs. control at respective day.

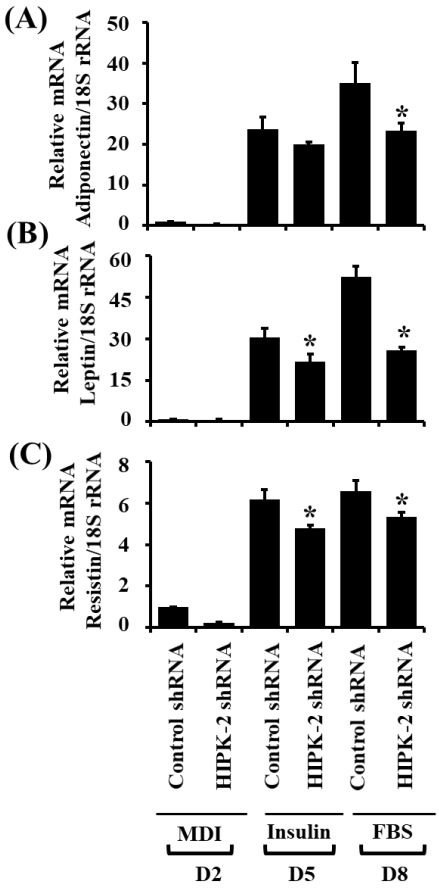

Figure 6. Effects of gene silencing of HIPK-2 on expression of leptin, adiponectin, and resistin during 3T3-L1 preadipocyte differentiation. (A,B,C) 3T3-L1 preadipocytes were stably transfected with 1 μg of control or HIPK-2 shRNA. Control or HIPK-2 shRNA-transfected cells were differentiated with an induction medium containing MDI, insulin, and FBS, and harvested at day 0 (D0), D2, D5, and D8, respectively. At each time point, total RNA was extracted and analyzed by real-time qPCR with respective primers. Data are mean ± SE (n=3). *$p<0.05$ vs. control at respective day.

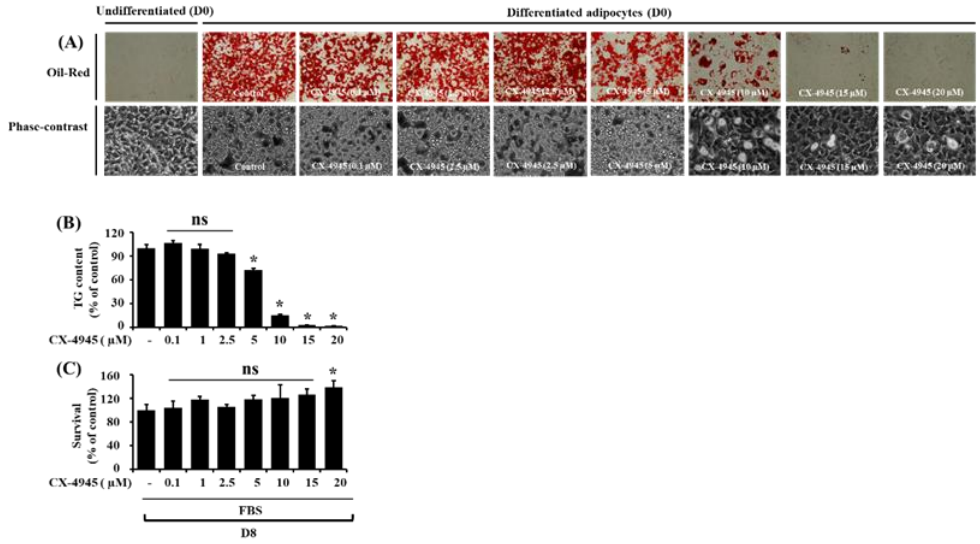

Figure 7. Effects of CX-4945, an inhibitor of HIPK-2, on lipid accumulation and cell survival during 3T3-L1 preadipocyte differentiation. (A) 3T3-L1 preadipocytes were induced to differentiate with an induction medium containing MDI, insulin, and FBS in the presence or absence of different concentrations of CX-4945 up to D8 of differentiation. On D8, cellular lipid contents were assessed by Oil Red O staining (upper panel) and phase-contrast images (lower panel) of the cells after the treatment. (B,C) On D8, cellular TG contents (B) and cell survival assay (C) were performed, respectively. Data are mean ± SE (n=3). *p<0.05 vs. control (D8).

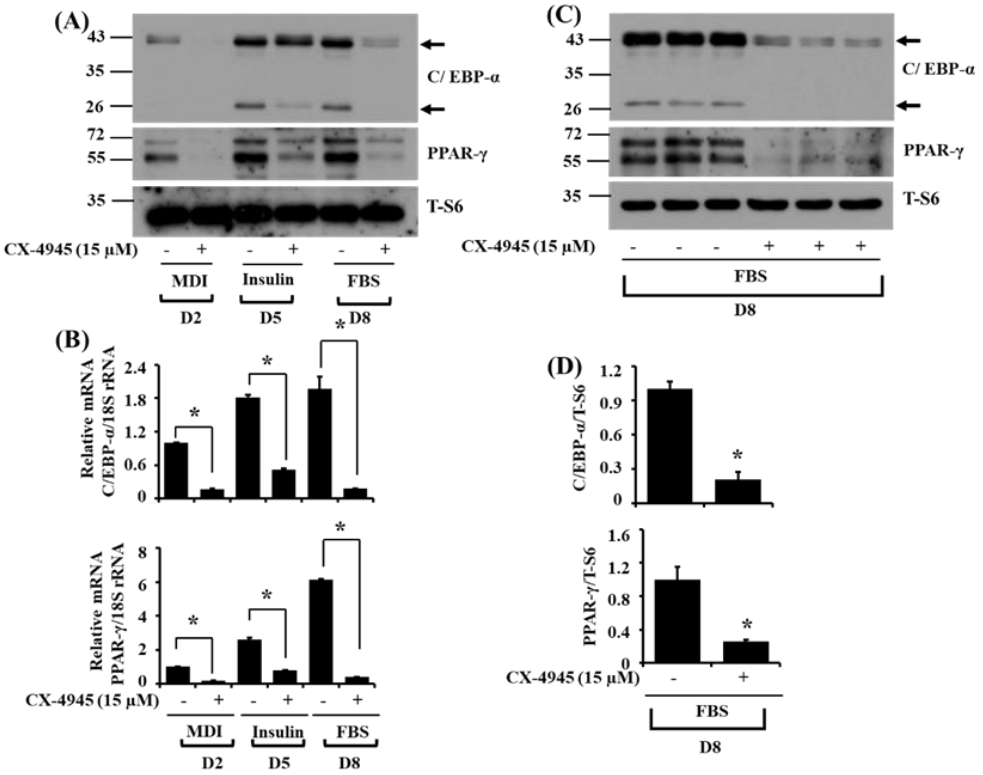

Figure 8. Effects of CX-4945, an inhibitor of HIPK-2, on expression of C/EBP-α and PPAR-γ during 3T3-L1 preadipocyte differentiation. (A,B) 3T3-L1 preadipocytes were induced to differentiate with an induction medium containing MDI, insulin, and FBS in the presence or absence of CX-4945 (15 μM), and harvested on D2, D5, and D8, respectively. At each time point, whole-cell lysates or total RNA was extracted and analyzed by immunoblot analysis (A) and real-time qPCR (B), respectively. Data are mean ± SE (n=3). *p<0.05 vs. control at respective day. (C,D) Western blot analysis in triplicate experiments on D8 (C) and densitometry data of (C) in (D). *p<0.05 vs. control (D8).

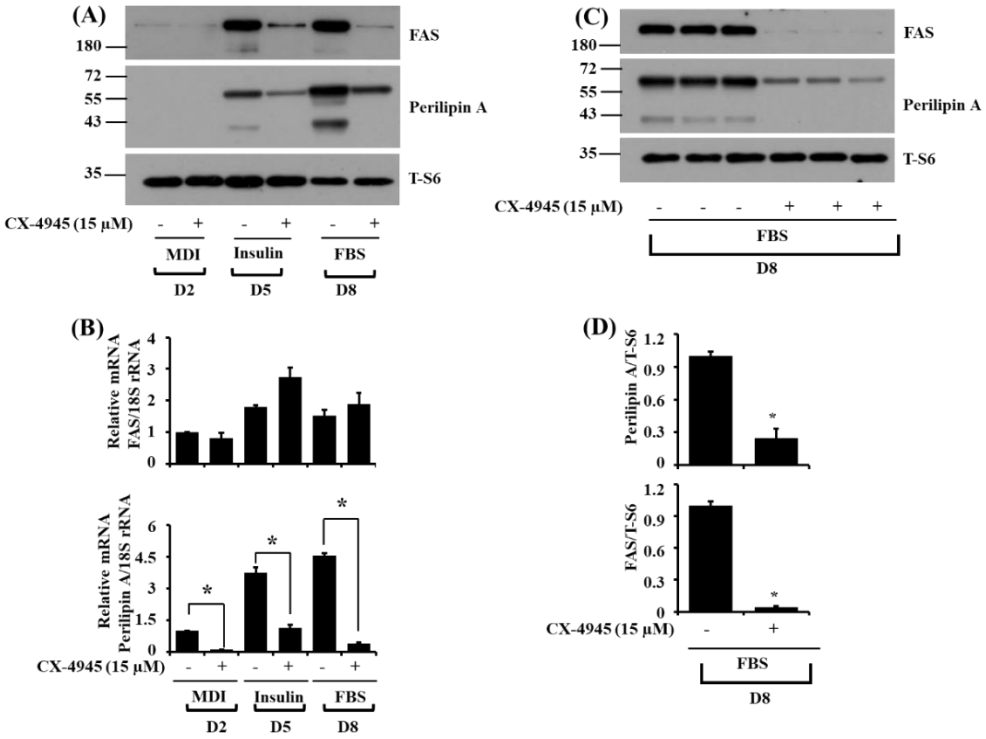

Figure 9. Effects of CX-4945, an inhibitor of HIPK-2, on expression of FAS and perilipin A during 3T3-L1 preadipocyte differentiation. (A,B) 3T3-L1 preadipocytes were induced to differentiate with an induction medium containing MDI, insulin, and FBS in the presence or absence of CX-4945 (15 μM), and harvested on D2, D5, and D8, respectively. At each time point, whole-cell lysates or total RNA was extracted and analyzed by immunoblot analysis (A) and real-time qPCR (B), respectively. Data are mean ± SE (n=3). *p<0.05 vs. control at respective day. (C,D) Western blot analysis in triplicate experiments on D8 (C) and densitometry data of (C) in (D). *p<0.05 vs. control (D8).

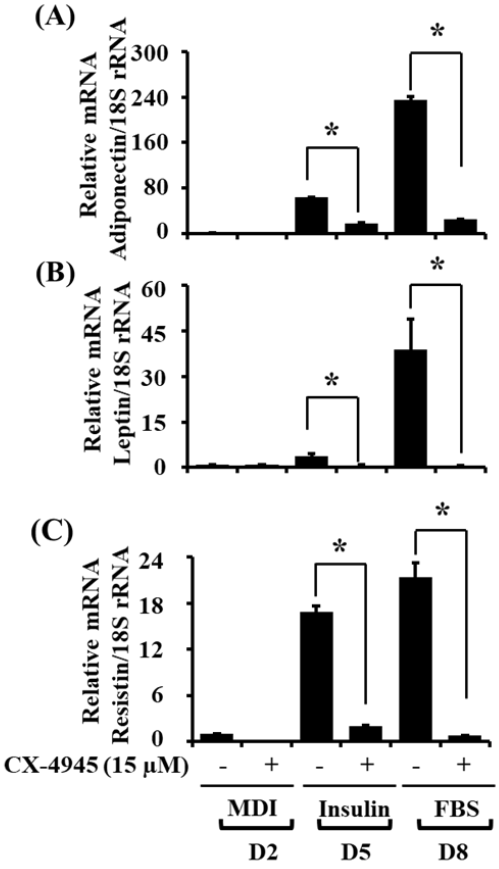

Figure 10. Effects of CX-4945, an inhibitor of HIPK-2, on expression of leptin, adiponectin, and resistin during 3T3-L1 preadipocyte differentiation. (A,B,C) 3T3-L1 preadipocytes were induced to differentiate with an induction medium containing MDI, insulin, and FBS in the presence or absence of CX-4945 (15 μM) and harvested on D2, D5, and D8, respectively. At each time point, total RNA was extracted and analyzed by real-time qPCR with respective primers. Data are mean ± SE (n=3). *$p<0.05$ vs. control at respective day.

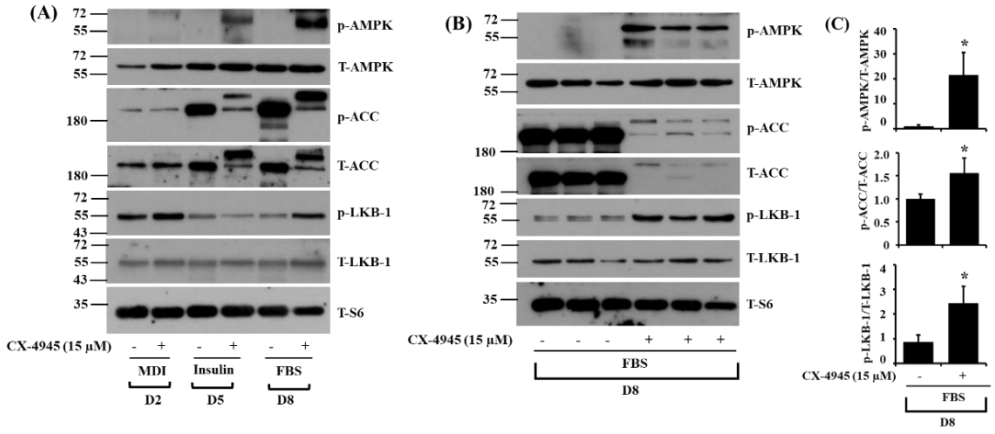

Figure 11. Effects of CX-4945, an inhibitor of HIPK-2, on expression and/or phosphorylation of AMPK, ACC, and LKB-1 during 3T3-L1 preadipocyte differentiation. (A) 3T3-L1 preadipocytes were induced to differentiate with an induction medium containing MDI, insulin, and FBS in the presence or absence of CX-4945 (15 μM) and harvested on D2, D5, and D8, respectively. At each time point, whole-cell lysates were prepared and analyzed by immunoblot analysis with respective antibodies. (B,C) Western blot analysis in triplicate experiments on D8 (B) and densitometry data of (B) in (C). *$p<0.05$ vs. control (D8).

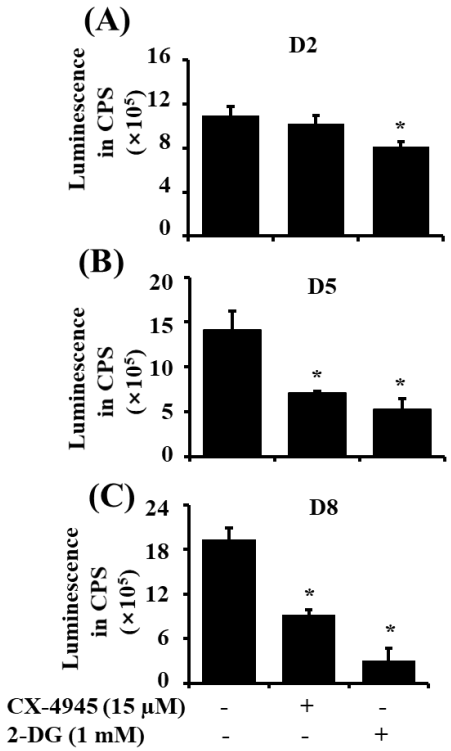

Figure 12. Effects of CX4945, an inhibitor of HIPK-2, on intracellular levels of ATP during 3T3-L1 preadipocyte differentiation. (A,B,C) 3T3-L1 preadipocytes were induced to differentiate with induction medium containing MDI, insulin, and FBS in the absence or presence of CX-4945 or 2-deoxyglucose (2-DG), a known ATP depleting agent, and harvested at D2 (A), D5 (B), and D8 (C), respectively. The amounts of intracellular ATP at the indicated timepoint were measured by an ATP measurement kit. Data are mean ± SE (n=3). *$p<0.05$ vs. control at respective day.

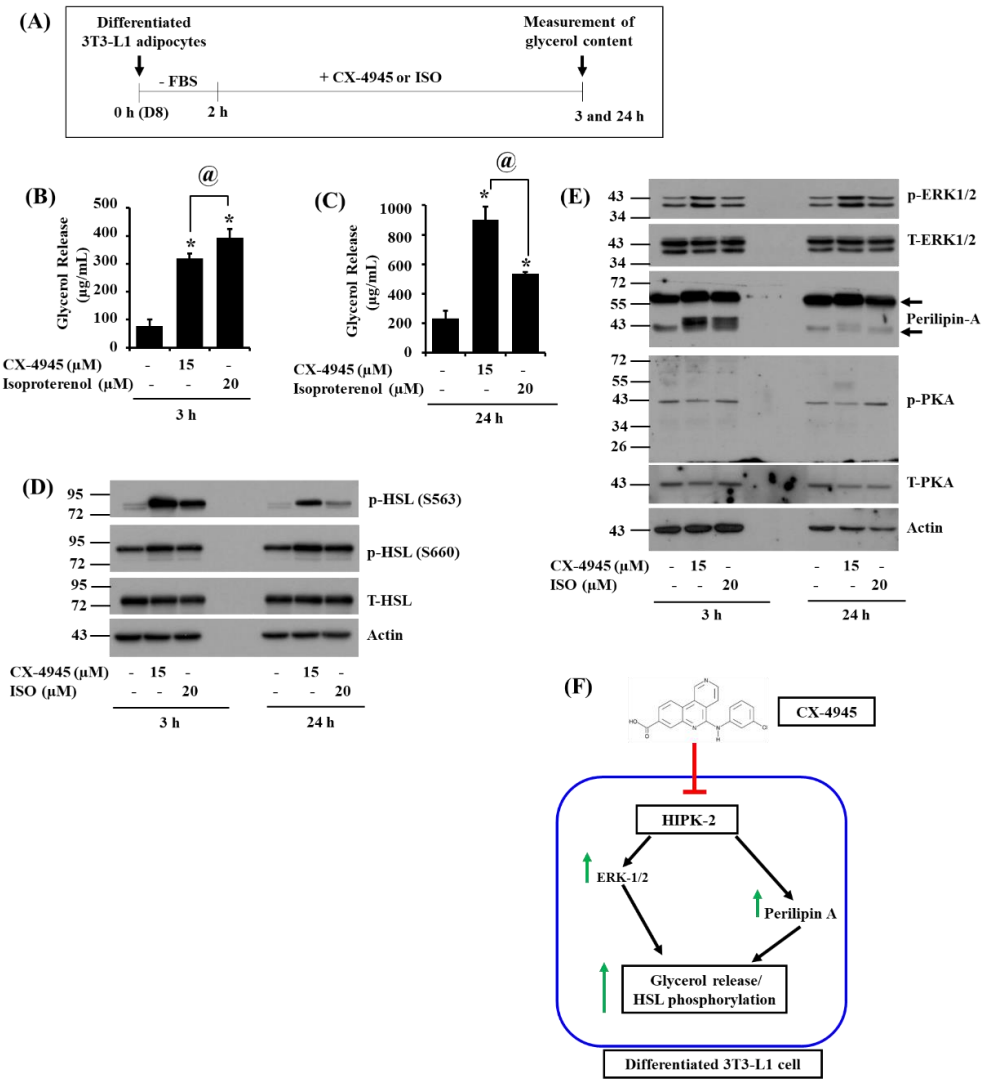

Figure 13. Effects of CX-4945, an inhibitor of HIPK-2, on lipolysis and expression and/or phosphorylation of HSL, ERK-1/2, perilipin A, and PKA during 3T3-L1 preadipocyte differentiation (A) The experimental scheme for the measurement of glycerol content and HSL phosphorylation in differentiated 3T3-L1 cells. (B,C) Differentiated 3T3-L1 cells were serum-starved for 2 h and treated with CX-4945

or ISO for indicated time points. Glycerol contents were measured at 3 h (A) and 24 h (B), respectively. Data are mean ± SE (n=3). *p<0.05 vs. control (3 or 14 h). (D,E) After-above mentioned treatment conditions, the cellular protein was extracted and analyzed by Western blot analysis with respective antibodies. (F) Graphical summary of Figure (E).

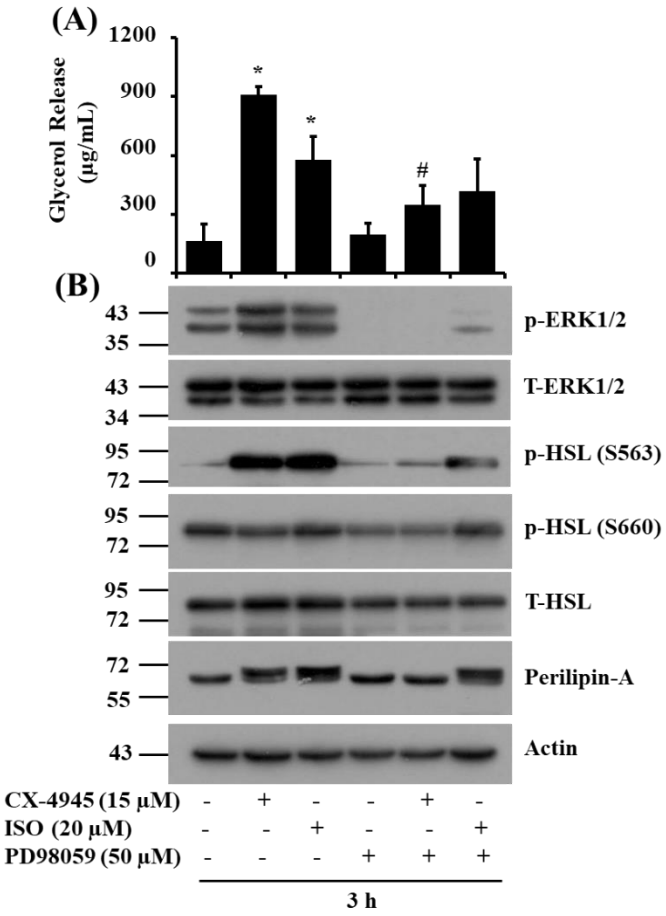

Figure 14. Effect of PD98059, an inhibitor of ERK-1/2, on CX-4945-induced lipolysis in differentiated 3T3-L1 cells. (A) Differentiated 3T3-L1 cells were serum-starved for 2 h and treated with CX-4945 or ISO in the presence or absence of PD98059 for 3 h. Glycerol content was measured at the indicated time point. Data are mean ± SE (n=3). *$p<0.05$ vs. control (no drug). (B) After the above-mentioned treatment conditions, the cellular protein was extracted and analyzed by Western blot analysis with respective antibodies.

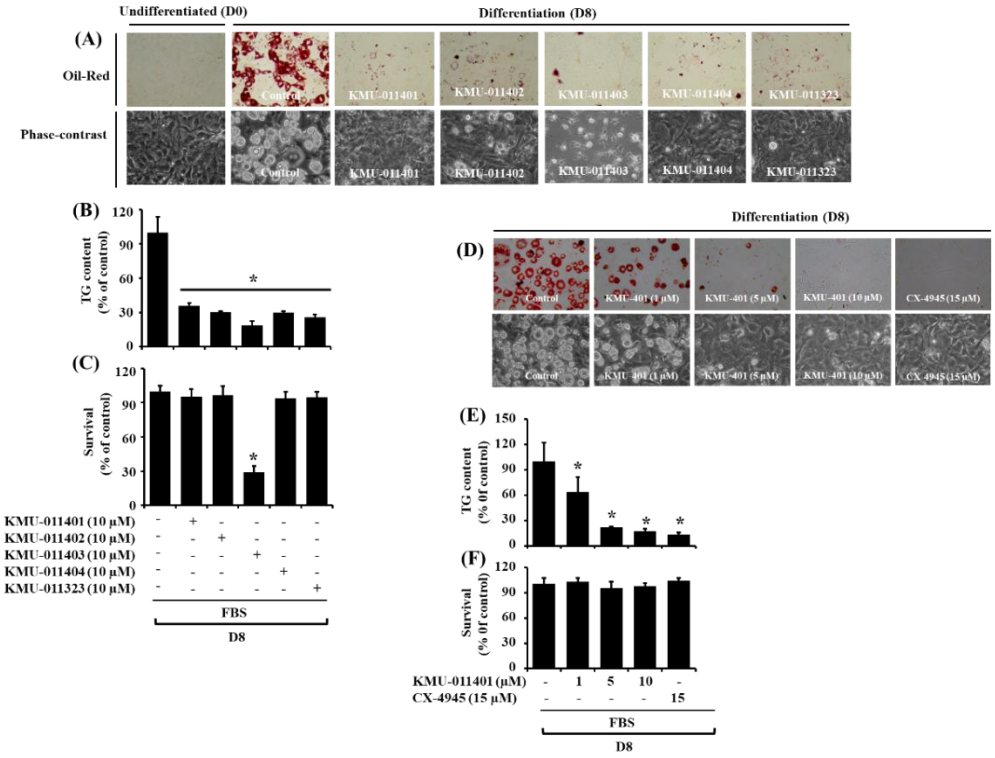

Figure 15. Effects of KMU-011401, KMU-011402, KMU-011403, KMU-011404, and KMU-011323, a series of novel HIPK-2 inhibitors, on lipid accumulation and cell survival in differentiating 3T3-L1 cells. (A) 3T3-L1 preadipocytes were induced to differentiate with induction medium in the presence or absence of different HIPK-2 inhibitors (KMU-011401, KMU-011402, KMU-011403, KMU-011404 KMU-011401323) up to D8 of differentiation. On D8, cellular lipid contents were assessed by Oil Red O staining (upper panel) and phase-contrast images (lower panel) of the cells after the treatment. (B,C) On D8, cellular TG contents (B) and cell survival assay (C) were performed, respectively. Data are mean ± SE (n=3). *p<0.05 vs. control (D8). (D) 3T3-L1

preadipocytes were induced to differentiate with induction medium in the presence or absence of different concentrations (1, 5, and 10 μM) of KMU-011401 and CX-4945 (15 μM) up to D8 of differentiation. On D8, cellular lipid contents were assessed by Oil Red O staining (upper panel) and phase-contrast images (lower panel) of the cells after the treatment. (E,F) On D8, cellular TG contents (E) and cell survival assay (F) were performed, respectively. Data are mean ± SE (n=3). *$p<0.05$ vs. control (D8).

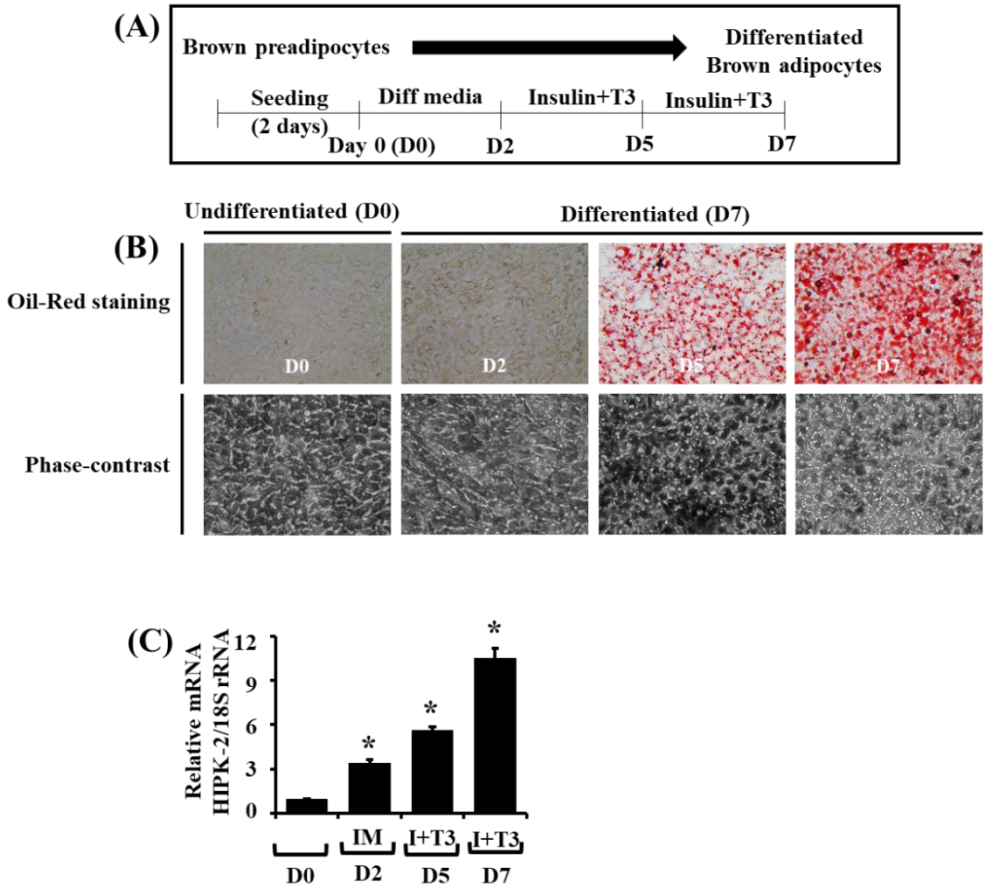

Figure 16. Lipid accumulation and expression of HIPK-2 during brown preadipocyte differentiation. (A) Experimental scheme for brown preadipocyte differentiation. (B) Measurement of lipid droplets accumulation on day 0 (D0), D2, D5, and D7 of brown preadipocyte differentiation by Oil Red O staining (upper panels) and by phase-contrast image (lower panels). (C) Brown preadipocytes were differentiated with induction medium and harvested at D0, D2, D5, and D7, respectively. At each time point, total cellular RNA was extracted and analyzed by real-time qPCR

with respective primers. Data are mean ± SE (n=3). *p<0.05 vs. control (D0).

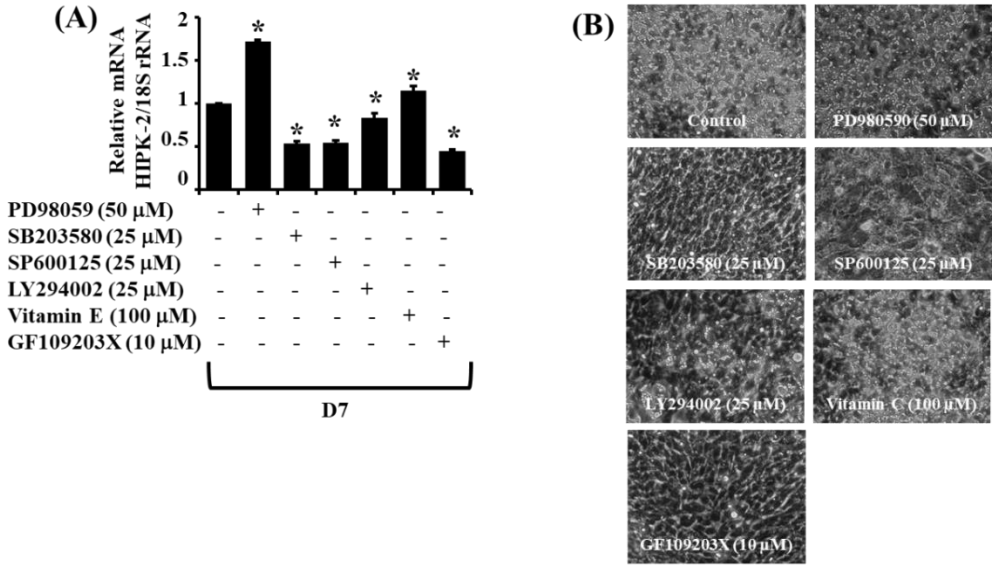

Figure 17. Effects of SB203580, PD98059, SP600125, LY294002, vitamin E or GF109203X on expression of HIPK-2 on D7 of brown preadipocyte differentiation. (A,B) Brown preadipocytes were differentiated with induction medium in the absence (control; 0.1 % DMSO) or presence of SB203580 (a p38 MAPK inhibitor), PD98059 (a MEK-1/2 (ERK-1/2) inhibitor), SP600125 (a JNK-1/2 inhibitor), LY294002 (a PI3K/PKB inhibitor), vitamin E (an antioxidant) or GF109203X (a PKC inhibitor) at designated concentrations, and harvested at day 7 (D7). Total cellular RNA was then extracted and analyzed by real-time qPCR with respective primers (A) and cellular lipid contents were assessed phase-contrast images after the treatment (B). Data are mean ± SE (n=3). *$p<0.05$ compared to the value of vehicle control.

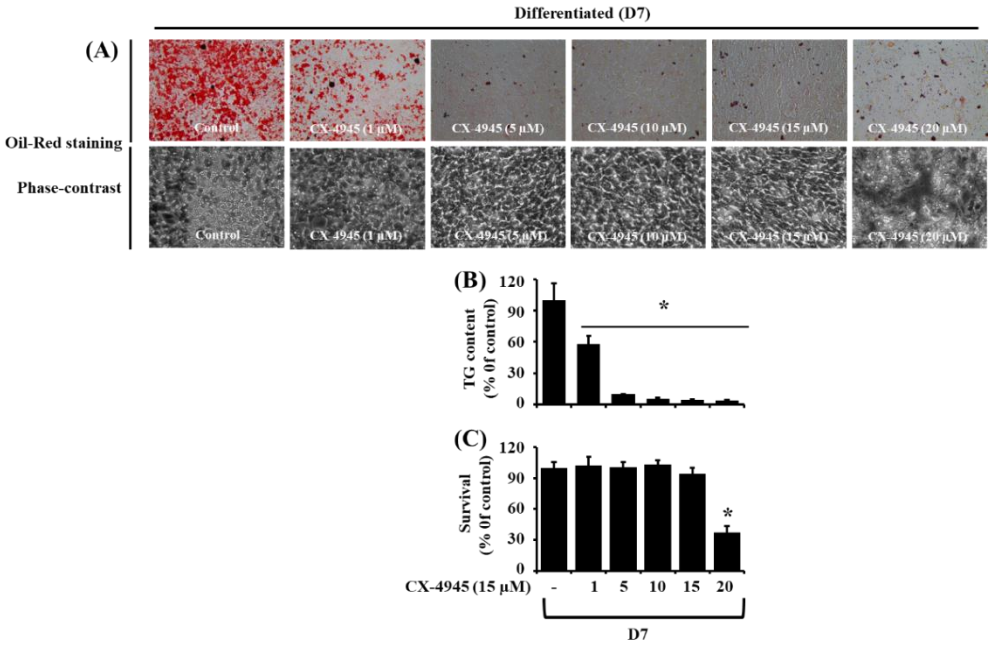

Figure 18. Effects of CX-4945, an inhibitor of HIPK-2, on lipid accumulation and cell survival during brown preadipocyte differentiation. (A) Brown preadipocytes were induced to differentiate with induction medium in the presence or absence of different concentrations of CX-4945 up to D7 of differentiation. On D7, cellular lipid contents were assessed by Oil Red O staining (upper panel) and phase-contrast images (lower panel) of the cells after the treatment. (B,C) On D7, cellular TG contents (B) and cell survival assay (C) were performed, respectively. Data are mean ± SE of three independent experiments. *p<0.05 vs. control (D7).

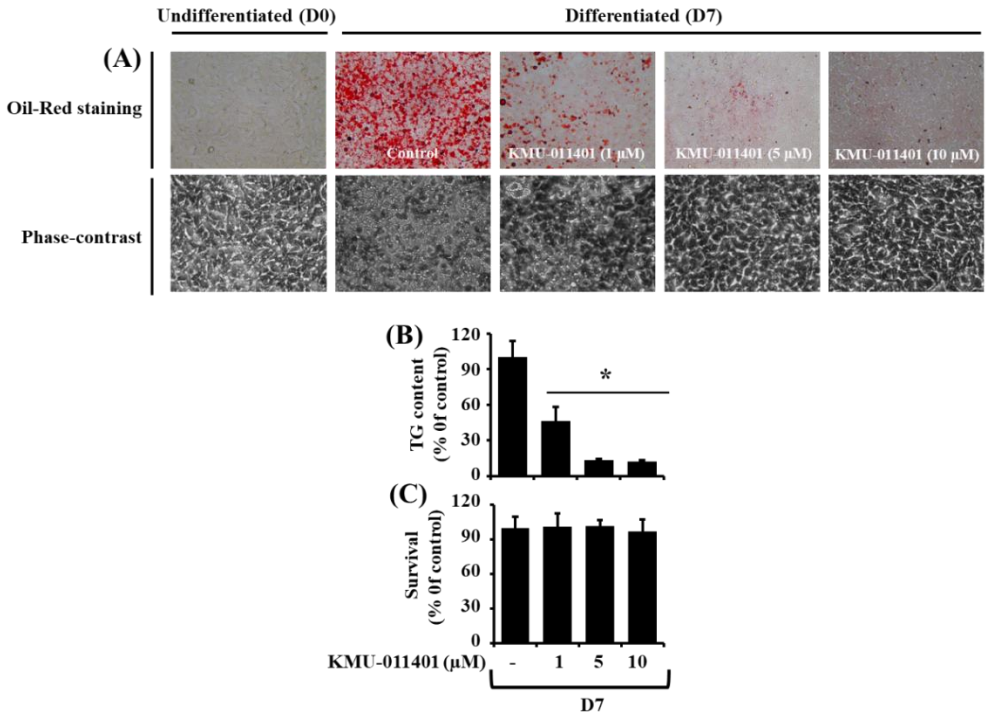

Figure 19. Effects of KMU-011401, a novel HIPK-2 inhibitor, on lipid accumulation, TG content, and cell survival during brown preadipocyte differentiation. (A) Brown preadipocytes were induced to differentiate with induction medium in the presence or absence of different concentrations of KMU-011401 up to D7 of differentiation. On D7, cellular lipid contents were assessed by Oil Red O staining (upper panel) and phase-contrast images (lower panel) of the cells after the treatment. (B,C) On D7, cellular TG contents (B) and cell survival assay (C) were performed, respectively. Data are mean ± SE of three independent experiments. *$p<0.05$ vs. control (D7).

4. Discussion

Excessive preadipocyte differentiation and the resultant high fat accumulation in the adipose tissue are closely linked to the development of obesity. Aforementioned, HIPK-2 has been implicated in the control and regulation of several transcription factors which play a pivotal role in embryonic development, apoptosis, cell proliferation, and tumor development (31, 33-36). Recent evidence has further indicated that HIPK-2 is an essential regulator of adipocyte differentiation and adipose tissue development *in vivo* and *in vitro* (40). However, until now, the expression regulation and role of HIPK-2 in white and brown adipocytes in the context of adipogenesis, adipogenesis, lipolysis, are still largely unknown. This study demonstrated that HIPK-2 expression is highly up-regulated during the murine 3T3-L1 white and brown preadipocyte differentiation in p38 MAPK and PKC-dependent manners, and the up-regulated HIPK-2 played a pivotal role in lipid accumulation and storage during murine white and brown preadipocytes differentiation. Gene silencing and pharmacological inhibition of HIPK-2 by CX-4945 and KMU-011401 resulted in not only a strong inhibition of lipid accumulation during murine 3T3-L1 white and brown preadipocyte differentiation but also a strong pro-lipolytic effect on differentiated or mature 3T3-L1 adipocytes, which are mediated through control of the expression and phosphorylation of C/EBP-α, PPAR-ɣ, STAT-3, FAS, ACC, perilipin A, AMPK, and HSL. This work suggests that HIPK-2 inhibition (inhibitor) may be used as potential preventive and therapeutics against obesity.

Studies have previously reported that HIPK-2 expression is high in both white adipose tissue (WAT) and brown adipose tissue (BAT) in mice (40). There is further evidence that HIPK-2 expression is low in 3T3-L1 preadipocytes, but its expression is vastly increased in differentiated or mature adipocytes, suggesting a link between HIPK-2 overexpression and white preadipocyte differentiation. Up to date, there is no information regarding HIPK-2 expression during brown preadipocyte differentiation. In this study, HIPK-2 expression was found to be highly elevated during the differentiation of both 3T3-L1 white preadipocytes and immortalized brown preadipocytes into mature white and brown adipocytes. These results further indicated a link between HIPK-2 overexpression and brown preadipocyte differentiation.

However, until now, the molecular and signaling mechanism of how HIPK-2 expression is regulated during white and brown preadipocyte differentiation remains unclear. Of note, data of pharmacological inhibition study performed in the current study evidently demonstrated that the mRNA expression of HIPK-2 during 3T3-L1 white preadipocyte differentiation was greatly repressed in the presence of SB203580 (a p38 MAPK inhibitor), GF109203X (a PKC inhibitor), SP600125 (a JNK-1/2 inhibitor) or LY294002 (a PI3K/PKB inhibitor). SB203580, GF109203X, SP600125, or LY294002 was not cytotoxic to 3T3-L1 white preadipocytes during differentiation. These results advocate that the activities of p38 MAPK, PKC, JNK-1/2, and PI3K/PKB are crucial for the transcriptional induction of HIPK-2 during 3T3-L1 preadipocyte differentiation. Furthermore, the mRNA expression of HIPK-2 during immortalized brown preadipocyte differentiation was largely suppressed in the presence of GF109203X, SB203580, or LY294002. In

this study, SP600125 at the dose tested herein was highly cytotoxic to immortalized brown preadipocytes during differentiation. It will be interesting to see the effect of SP600125 at lower doses on transcriptional regulation of HIPK-2 in brown preadipocytes. These results thus point out that the activities of PKC, p38 MAPK, and PI3K/PKB are important for the transcriptional induction of HIPK-2 during brown preadipocyte differentiation. There is also a wealth of information illustrating that expression of HIPK-2 is regulated at post-transcription (mRNA stability), translation, protein stability, and post-translation modification (PTM) (51, 52). Given that p38 MAPK, PKC, JNK-1/2, and PI3K/PKB also participate in the regulation of post-transcription (mRNA stability), translation, protein stability, and PTM of many proteins (53-55), it will be interesting to investigate, in the future, their role in mRNA stability, translation, protein stability, and/or PTM of HIPK-2 during white and brown preadipocyte differentiation.

Recent *in vitro* and *in vivo* studies have demonstrated that loss of HIPK-2 specifically inhibits white adipocyte differentiation and tissue development (40). Furthermore, it has been shown that gene silencing of HIPK-2 leads to inhibition of lipid accumulation during 3T3-L1 white preadipocyte differentiation (40). In the present study, knock-down of HIPK-2 was found to result in not only suppression of lipid accumulation but also reduction of TG content during 3T3-L1 white preadipocyte differentiation. These results evidently indicate the stimulatory role of HIPK-2 expression and activity in adipogenesis and lipogenesis during 3T3-L1 white preadipocyte differentiation. Until now, the molecular and signaling mechanism of how HIPK-2

stimulates adipogenesis and lipogenesis in the 3T3-L1 white preadipocyte differentiation process is not fully defined.

A large body of evidence strongly supports the pivotal role of numerous transcription factors, such as C/EBP-α, PPAR-ɣ, and STAT-3, in 3T3-L1 white preadipocyte differentiation (16-19). At present, HIPK-2 regulation of C/EBP-α, PPAR-ɣ, and STAT-3 during 3T3-L1 white preadipocyte differentiation is unknown. Thus, the effect of knock-down of HIPK-2 on expression and/or phosphorylation of C/EBP-α, PPAR-ɣ, and STAT-3 in 3T3-L1 white preadipocyte differentiation process was further investigated in the present study. Of interest, gene silencing of HIPK-2 was found to strongly repress expression of C/EBP-α and PPAR-ɣ at both protein and mRNA levels in the 3T3-L1 white preadipocyte differentiation process. These results address that HIPK-2 expression and activity are necessary for the transcriptional up-regulation of C/EBP-α and PPAR-ɣ in the cell differentiation process. Previous studies have demonstrated that HIPK-2 directly interacts and cooperates with C/EBP-β and p300, a transcriptional co-activator, at the protein levels, and this is functionally relevant and crucial for adipocyte differentiation of 3T3-L1 cells (39). However, at this moment, it is unclear how HIPK-2 controls the transcription of C/EBP-α and PPAR-ɣ during the 3T3-L1 white preadipocyte differentiation process. Considering that HIPK-2 directly interacts and cooperates with C/EBP-β, and C/EBP-β is involved in the transcriptional up-regulation of C/EBP-α and PPAR-ɣ during the 3T3-L1 white preadipocyte differentiation process (39, 56), it will be interesting to test, in the future, whether gene silencing of HIPK-2 leads to the reduced expression and/or transcriptional activity of C/EBP-β during 3T3-L1 white preadipocyte

differentiation process or knock-down of C/EBP-β causes the transcriptional repression of C/EBP-α and PPAR-γ during the cell differentiation process.

Previously, it has also been reported that the family of STATs, including STAT-1, STAT-3, STAT-5, and STAT-6, are expressed in both 3T3-L1 preadipocytes and adipocytes and critical for 3T3-L1 adipocyte differentiation (19). Recently, it has been reported that HIPK-2 is a positive regulator of the JAK/STAT pathway during the development and tumorigenesis (57). This notion is further supported by that the transcriptional output of JAK/STAT signaling is perturbed upon loss or knock-down of HIPK-2 and conversely increased HIPK-2 induces elevated JAK/STAT activity including STAT-3 in a cell-autonomous manner (58). In the current study, genetic silencing of HIPK-2 was found to partially interfere with STAT-3 phosphorylation without altering total STAT-3 protein levels on D5 and D8 of 3T3-L1 preadipocyte differentiation, pointing out that HIPK-2 knock-down caused the reduced phosphorylation of pre-existed STAT-3 protein without de novo protein synthesis. These results collectively indicated that HIPK-2 expression and activity also facilitate the elevated phosphorylation of STAT-3 in these cell differentiation processes, and thus inhibition of lipid accumulation by knock-down of HIPK-2 is in part due to the reduced phosphorylation of STAT-3.

It has been well documented that expression of both FAS and perilipin A are largely increased in a time-dependent manner during 3T3-L1 preadipocyte differentiation (20,22). FAS is a crucial lipogenic enzyme that catalyzes intermediate steps in the biosynthesis of long-chain fatty acids and its overexpression leads to an induce fatty acid biosynthesis in cells and/or tissues (20, 59). Perilipin A binds

to and stabilizes the newly formed LDs during 3T3-L1 preadipocyte differentiation (22). Strong pieces of evidence also indicate that perilipin A is a highly phosphorylated protein in adipocytes that is not secreted but localized at the surface of LDs (22,60). It also has been illustrated that perilipin A expression in human adipose tissue is elevated with obesity (22). Considering the role of FAS and perilipin A in lipogenesis and LDs-stabilization and storage in adipocytes, blockage of the activity and/or expression of FAS and perilipin A is likely to be another possible way to prevent or treat obesity at the cellular context of lipogenesis and LDs metabolism. Little is known about HIPK-2 regulation of FAS and perilipin A expression in adipocytes. Notably, in this study, knock-down or pharmacological inhibition of HIPK-2 by CX-4945 led to the decreased or slight induction in the expression of FAS during 3T3-L1 preadipocytes differentiation, respectively. At the same time, knock-down or pharmacological inhibition of HIPK-2 by CX-4945 reduced the perilipin A at the protein and mRNA levels during the 3T3-L1 preadipocyte differentiation process. These results point out that HIPK-2 expression plays a crucial role in the transcriptional and translational up-regulation of FAS and perilipin A in the 3T3-L1 preadipocyte differentiation process, and thus suppression of lipid accumulation by knock-down of HIPK-2 herein is closely linked to the reduced expression of FAS and perilipin A.

Adipocytes, the most abundant cell type in adipose tissue, are a major source of adipokines including adiponectin, leptin, and resistin (11-13). Reportedly, while adiponectin expression levels decrease with an increase in adiposity (61), leptin and resistin levels increase in obesity (62). The adipocytes-derived hormone resistin is

postulated to be linked to obesity, insulin resistance, and diabetes (63). Consequently, suppression of adipokines such as leptin or resistin expression is an alternative against obesity. In this study, knock-down of HIPK-2 was found to inhibit the expression of adiponectin, leptin, and resistin at the mRNA levels during the 3T3-L1 preadipocyte differentiation process. These results suggest that HIPK-2 expression and activity are crucial for the transcriptional up-regulation of these adipokines in the 3T3-L1 preadipocyte differentiation process.

Recently, it has been demonstrated that CX-4945 strongly interacts with the residues in the ATP-pocket of HIPK-2 and blocks its catalytic activity (41), indicating that CX-4945 is an inhibitor of HIPK-2. In the present study, pharmacological inhibition of HIPK-2 using CX-4945, not only strongly suppressed lipid accumulation but also reduction of TG content without affecting the survival of 3T3-L1 preadipocytes. These results indicated that blockage of the kinase activity of HIPK-2 impinges adipogenesis and lipogenesis during 3T3-L1 preadipocyte differentiation.

Several studies have exhibited the crucial roles of several numerous transcription factors, such as C/EBP-α, PPAR-γ, and STAT-3, in 3T3-L1 white preadipocyte differentiation (16-19). At present, HIPK-2 regulation of C/EBP-α, PPAR-γ, and STAT-3 during 3T3-L1 white preadipocyte differentiation is unknown. Thus, the effect of CX-4945 on expression and/or phosphorylation of C/EBP-α and PPAR-γ in the 3T3-L1 white preadipocyte differentiation process was further investigated in the present study. Notably, CX-4945 greatly represses the expression of C/EBP-α and PPAR-γ at both protein and mRNA levels in the 3T3-L1 white preadipocyte differentiation process. These

results further supported that HIPK-2 expression is necessary for the transcriptional up-regulation of C/EBP-α and PPAR-ɣ in the cell differentiation process, and thus inhibition of lipid accumulation by pharmacological inhibition of HIPK-2 by CX-4945 is largely attributable to the reduced expression of C/EBP-α and PPAR-ɣ at their transcript levels herein.

Adipokines including adiponectin, leptin, and resistin are mainly secreted from Adipose tissue and adipocytes and their expressions were increased in obesity. Reportedly, while adiponectin expression levels decrease with an increase in adiposity (61), leptin and resistin levels increase in obesity (62). The adipocytes-derived hormone resistin is postulated to be linked to obesity, insulin resistance, and diabetes (63). Consequently, suppression of leptin and resistin expression is an alternative against obesity. In this study, CX-4945 strongly decreased the expression of adiponectin, leptin, and resistin at the mRNA levels during the 3T3-L1 preadipocyte differentiation process indicating that the HIPK-2 expression and activity are crucial for the transcriptional up-regulation of these adipokines in the 3T3-L1 preadipocyte differentiation process.

AMPK is the master regulator of energy metabolism and balance (64). It is a heterotrimeric protein kinase consisting of a catalytic a subunit and regulatory b and c subunits. Current research has shown that elevation of intracellular AMP/ATP induces AMPK phosphorylation on T172 within a subunit by liver kinase B1 (LKB1) (65). Several studies have reported that phosphorylation (activation) of AMPK blocks ATP-consuming anabolic processes while activates ATP-producing catabolic processes (66,67) and the effects are mediated via the phosphorylation of metabolic enzymes, such as ACC (68). There is also

evidence that activation of AMPK induces ACC phosphorylation on S79, which strictly regulates the enzyme during fatty acid synthesis for malonyl-CoA production, and phosphorylated ACC lacks its activity to synthesize fatty acids (69). At present, HIPK-2 regulation of phosphorylation/or expression of AMPK, ACC, and LKB-1 during 3T3-L1 white preadipocyte differentiation is unknown. Given that CX-4945 increases phosphorylation/expression of AMPK and ACC in differentiating 3T3-L1 cells, the drug's anti-adipogenic effect is further mediated through activation of AMPK and ACC, which may confer inhibition of ATP-consuming anabolic processes, such as synthesis of fatty acids. Furthermore, in this study, CX-4945 increased LKB-1 phosphorylation while lowered cellular ATP levels in differentiating 3T3-L1 cells. These results indicate that CX-4945-induced AMPK phosphorylation is in part due to LKB-1 activation and reduction of cellular ATP levels during the differentiation of 3T3-L1 cells.

Lipolysis involves the hydrolytic cleavage of ester bonds in triacylglyceride (TG), resulting in the formation of free fatty acids and glycerol as a byproduct (28). Hormone-sensitive lipases (HSL) is a pivotal enzyme that involves the mobilization of fatty acids from stored TG (28). Previous research stated that activation of protein kinase A and/or extracellular signal-related kinase (ERK) induces lipolysis via phosphorylating HSL on S563, S659, and S660 in adipocytes (29,30). At present, HIPK-2 regulation of glycerol release and expression/or phosphorylation of HSL, perilipin A, ERK-1/2, and PKA in differentiated 3T3-L1 is unknown. Herein, we observed that pharmacological inhibition of HIPK-2 by CX-4945 has a lipolytic effect on differentiated 3T3-L1 cells as demonstrated by elevation of glycerol release as well as phosphorylation of HSL at S563 and S659.

Furthermore, treatment with CX-4945 induced the phosphorylation of ERK-1/2 along with an electrophoretic shift (hyperphosphorylation) in perilipin A protein expressions. Notably, inhibition of ERK-1/2 by PD98059, a MEK-1/2 inhibitor, significantly impeded the CX-4945-induced lipolysis, indicating CX-4945 exerts its lipolytic effect via the ERK1/2-dependent HSL activation.

Due to the very limited commercial availability of HIPK-2 inhibitors, a series of novel HIPK-2 inhibitors (KMU-011401, KMU-011402, KMU-011403, KMU-011404, and KMU-011323) were herein synthesized by medicinal chemistry. In this study, all HIPK-2 inhibitors (KMU-011401, KMU-011402, KMU-011403, KMU-011404, and KMU-011323) tested strongly suppressed lipid accumulation as well as TG content during 3T3-L1 preadipocyte differentiation. However, in this study, KMU-011403 at the dose tested herein was highly cytotoxic during the 3T3-L1 preadipocytes differentiation. Among these novel HIPK-2 inhibitors tested, KMU-011-401 most greatly blocked lipid accumulation and reduced TG content in a concentration-dependent manner with no cytotoxicity during the differentiation 3T3-L1 preadipocytes into adipocytes, supporting that the blockage of HIPK-2 activity by KMU-011401 and other HIPK-2 inhibitors applied impinges 3T3-L1 preadipocytes differentiation, which further repressed lipid accumulation during cell differentiation.

It has been well documented the HIPK-2 is actively involved in the appearance of brown/beige adipocytes in different adipose tissue depots via adipogenesis (40). However, the function of HIPK-2 in brown preadipocyte differentiation remains elusive. Strikingly, in this study, pharmacological inhibition of HIPK-2 with CX-4945 and KMU-011401, results in a strong reduction of lipid accumulation and TG

content with no cytotoxicity during brown preadipocyte differentiation, illustrating that HIPK-2 also plays a role in lipid accumulation and storage in brown adipocytes.

It is evident that HIPK-2 expression is highly increased, and the increased HIPK-2 plays a pivotal role in lipid metabolism (lipid accumulation and lipolysis) in murine 3T3-L1 white and/or brown (pre)adipocytes. However, at this moment, it is unclear whether the increased HIPK-2 during murine 3T3-L1 white and brown (pre)adipocyte differentiation has kinase activity, because of no successful establishment of an *in vitro* model system to measure the kinase activity. It will be thus necessary to make an appropriate *in vitro* model system to verify if the increased HIPK-2 during murine 3T3-L1 white and brown (pre)adipocyte differentiation truly has kinase activity. It should be further noted that both the expression and role of HIPK-2 and the effect of HIPK-2 inhibitors in the regulation of lipid accumulation and/or lipolysis herein are seen in cultured murine white and brown (pre)adipocytes. Given that there is a big difference in not only regulation of lipid accumulation and lipolysis but also control of expression and activity of lipid accumulation and lipolysis-related transcription factors, enzymes, and proteins between mouse (pre)adipocytes and human ones, future studies are warranted to confirm whether 1) HIPK-2 expression is increased and the increased HIPK-2 plays a crucial role in lipid metabolism (lipid accumulation and lipolysis) human white and/or brown (pre)adipocytes, and 2) the treatment of HIPK-2 inhibitors blocks the differentiation of human white and brown preadipocytes, and 3) HIPK-2 expression is higher in white and brown adipocyte tissues of obese people or

patients than those of normal person, and 4) the administration of HIPK-2 inhibitors reduces the adiposity of obese people or patients.

5. Summary

In summary, the present study demonstrates that HIPK-2 expression is highly up-regulated during the murine 3T3-L1 white and brown preadipocyte differentiation in p38 MAPK and PKC-dependent manners, and the up-regulated HIPK-2 plays a pivotal role in lipid accumulation and storage during murine white and brown preadipocytes differentiation. Gene silencing and pharmacological inhibition of HIPK-2 by CX-4945 and KMU-011401 results in not only a strong inhibition of lipid accumulation during murine 3T3-L1 white and brown preadipocyte differentiation but also a strong pro-lipolytic effect on differentiated or mature 3T3-L1 adipocytes, which are mediated through control of the expression and phosphorylation of C/EBP-α, PPAR-ɣ, STAT-3, FAS, ACC, perilipin A, AMPK, and HSL. This work suggests that HIPK-2 inhibition (inhibitor) may be used as potential preventive and therapeutics against obesity.

References

1. Goran MI, Ball GD, Cruz ML: Obesity and risk of type 2 diabetes and cardiovascular disease in children and adolescents. J Clin Endocrinol Metab 2003; 88: 1417-27.

2. Blüher M: Obesity: global epidemiology and pathogenesis. Nat Rev Endocrinol 2019; 15: 288-98.

3. Hruby A, Hu FB: The Epidemiology of Obesity: A Big Picture. Pharmacoeconomics 2015; 33: 673-89.

4. Spiegelman BM, Flier JS: Obesity and the regulation of energy balance. Cell 2001; 104: 531-43.

5. Pi-Sunyer FX: The obesity epidemic: pathophysiology and consequences of obesity. Obes Res 2002; 2: 97S-104S.

6. Hill JO, Wyatt HR, Peters JC: Energy balance and obesity. Circulation 2012; 126: 126-32.

7. Ali AT, Hochfeld WE, Myburgh R, Pepper MS: Adipocyte and adipogenesis. Eur J Cell Biol 2013; 92: 229-36.

8. Kershaw EE, Flier JS: Adipose tissue as an endocrine organ. J Clin Endocrinol Metab 2004; 89: 2548-56.

9. Sheikh AB, Nasrullah A, Haq S, Akhtar A, Ghazanfar H, Nasir A, et al: The Interplay of Genetics and Environmental Factors in the Development of Obesity. Cureus. 2017; 9: e1435.

10. Rosen ED, Spiegelman BM: Adipocytes as regulators of energy balance and glucose homeostasis. Nature 2006; 444: 847-53.

11. Blüher M: Adipokines - removing road blocks to obesity and diabetes therapy. Mol Metab 2014; 3: 230-40.

12. Skurk T, Alberti-Huber C, Herder C, Hauner H: Relationship between adipocyte size and adipokine expression and secretion. J Clin Endocrinol Metab 2007: 92: 1023-33.

13. Zorena K, Jachimowicz-Duda O, Ślęzak D, Robakowska M, Mrugacz M: Adipokines and Obesity. Potential Link to Metabolic Disorders and Chronic Complications. Int J Mol Sci 2020; 21: 3570.

14. Jones JEC, Rabhi N, Orofino J, Gamini R, Perissi V, Vernochet C, Farmer SR: The Adipocyte Acquires a Fibroblast-Like Transcriptional Signature in Response to a High Fat Diet. Sci Rep 2020; 10: 2380.

15. Sarjeant K, Stephens JM: Adipogenesis. Cold Spring Harb Perspect Biol 2012; 4: a008417.

16. Farmer SR; Transcriptional control of adipocyte formation. Cell Metab 2006; 4: 263-73.

17. Cao Z, Umek RM, McKnight SL: Regulated expression of three C/EBP isoforms during adipose conversion of 3T3-L1 cells. Genes Dev; 5: 1538-52.

18. Lehrke M, Lazar MA: The many faces of PPARgamma. Cell 2005; 123: 993-99.

19. Burrell JA, Boudreau A, Stephens JM: Latest advances in STAT signaling and function in adipocytes. Clin Sci (Lond) 2020; 134: 629-39.

20. Lakshmanan MR, Nepokroeff CM, Porter JW: Control of the synthesis of fatty-acid synthetase in rat liver by insulin, glucagon, and adenosine 3':5' cyclic monophosphate. Proc Natl Acad Sci U S A 1972; 69: 3516-29.

21. Janovská A, Hatzinikolas G, Staikopoulos V, McInerney J, Mano M, Wittert GA: AMPK and ACC phosphorylation: effect of leptin, muscle fibre type and obesity. Mol Cell Endocrinol 2008; 284: 1-10.

22. Kern PA, Di Gregorio G, Lu T, Rassouli N, Ranganathan G: Perilipin expression in human adipose tissue is elevated with obesity. J Clin Endocrinol Metab 2004; 89: 1352-8.

23. Wolins NE, Brasaemle DL, Bickel PE: A proposed model of fat packaging by exchangeable lipid droplet proteins. FEBS Lett 2006; 580: 5484-91.

24. Lage R, Diéguez C, Vidal-Puig A, López M: AMPK: a metabolic gauge regulating whole-body energy homeostasis. Trends Mol Med 2008; 14: 539-49.

25. Martini CN, Plaza MV, Vila Mdel C: PKA-dependent and independent cAMP signaling in 3T3-L1 fibroblasts differentiation. Mol Cell Endocrinol 2009; 298: 42-7.

26. Prusty D, Park BH, Davis KE, Farmer SR: Activation of MEK/ERK signaling promotes adipogenesis by enhancing peroxisome proliferator-activated receptor gamma (PPARgamma) and C/EBPalpha gene expression during the differentiation of 3T3-L1 preadipocytes. J Biol Chem 2002; 277: 46226-32.

27. Engelman JA, Lisanti MP, Scherer PE: Specific inhibitors of p38 mitogen-activated protein kinase block 3T3-L1 adipogenesis. J Biol Chem 1998; 273: 32111-20.

28. Schweiger M, Eichmann TO, Taschler U, Zimmermann R, Zechner R, Lass A: Measurement of lipolysis. Methods Enzymol 2014; 538: 171-93.

29. Greenberg AS, Shen WJ, Muliro K, Patel S, Souza SC, Roth RA, Kraemer FB: Stimulation of lipolysis and hormone-sensitive lipase via the extracellular signal-regulated kinase pathway. J Biol Chem 2001; 276: 45456-61.

30. Krintel C, Mörgelin M, Logan DT, Holm C: Phosphorylation of hormone-sensitive lipase by protein kinase A in vitro promotes an

increase in its hydrophobic surface area. FEBS J 2009; 276: 4752-62.

31. Kim YH, Choi CY, Lee SJ, Conti MA, Kim Y: Homeodomain-interacting protein kinases, a novel family of co-repressors for homeodomain transcription factors. J Biol Chem 1998; 273: 25875-79.

32. Manning G, Whyte DB, Martinez R, Hunter T, Sudarsanam S: The protein kinase complement of the human genome. Science 2002; 298: 1912-34.

33. Saul VV, Schmitz ML: Posttranslational modifications regulate HIPK2, a driver of proliferative diseases. J Mol Med (Berl) 2013; 91: 1051-58.

34. Calzado MA, de la Vega L, Möller A, Bowtell DD, Schmitz ML: An inducible autoregulatory loop between HIPK2 and Siah2 at the apex of the hypoxic response. Nat Cell Biol 2009; 11: 85-91.

35. Nardinocchi L, Puca R, Guidolin D, Belloni AS, Bossi G, Michiels C, et al: Transcriptional regulation of hypoxia-inducible factor 1alpha by HIPK2 suggests a novel mechanism to restrain tumor growth. Biochim Biophys Acta 2009; 1793: 368-77.

36. Calzado MA, Renner F, Roscic A, Schmitz ML: HIPK2: a versatile switchboard regulating the transcription machinery and cell death. Cell Cycle 2007; 6: 139-43.

37. Hofmann TG, Glas C, Bitomsky N: HIPK2: A tumour suppressor that controls DNA damage-induced cell fate and cytokinesis. Bioessays 2013; 35: 55-64.

38. D'Orazi G, Rinaldo C, Soddu S: Updates on HIPK2: a resourceful oncosuppressor for clearing cancer. J Exp Clin Cancer Res 2012; 31: 63.

39. Steinmann S, Coulibaly A, Ohnheiser J, Jakobs A, Klempnauer KH: Interaction and cooperation of the CCAAT-box enhancer-binding protein β (C/EBPβ) with the homeodomain-interacting protein kinase 2 (Hipk2). J Biol Chem 2013; 288: 22257-69.

40. Sjölund J, Pelorosso FG, Quigley DA, DelRosario R, Balmain A: Identification of Hipk2 as an essential regulator of white fat development. Proc Natl Acad Sci U S A 2014; 111: 7373-8.

41. Agnew C, Liu L, Liu S, Xu W, You L, Yeung W, et al: The crystal structure of the protein kinase HIPK2 reveals a unique architecture of its CMGC-insert region. J Biol Chem 2019; 294: 13545-59.

42. Lage R, Dieguez C, Vidal-Puig A, Lopez M: AMPK: a metabolic gauge regulating whole-body energy homeostasis. Trends Mol Med 2008; 14: 539-49.

43. Abdel-Magid AF: Treatment of obesity and related disorders with acetyl-CoA carboxylase inhibitors. ACS Med Chem Lett 2013; 4: 16-17.

44. Xi P, Du J, Liang H, Han J, Wu Z, Wang H, et al: Intraventricular Injection of LKB1 Inhibits the Formation of Diet-Induced Obesity in Rats by Activating the AMPK-POMC Neurons-Sympathetic Nervous System Axis. Cell Physiol Biochem 2018; 47: 54-66.

45. Gowans GJ, Hardie DG: AMPK: a cellular energy sensor primarily regulated by AMP. Biochem Soc Trans 2014; 42: 71-5.

46. Zalatan F, Krause JA, Blask DE: Inhibition of isoproterenol-induced lipolysis in rat inguinal adipocytes in vitro by physiological melatonin via a receptor-mediated mechanism. Endocrinology 2001; 142: 3783-90.

47. Duncan RE, Ahmadian M, Jaworski K, Sarkadi-Nagy E, Sul HS: Regulation of lipolysis in adipocytes. Annu Rev Nutr 2007; 27: 79-101.

48. Zu L, He J, Jiang H, Xu C, Pu S, Xu G: Bacterial endotoxin stimulates adipose lipolysis via toll-like receptor 4 and extracellular signal-regulated kinase pathway. J Biol Chem 2009; 284: 5915-26.

49. Tansey JT, Sztalryd C, Hlavin EM, Kimmel AR, Londos C: The central role of perilipin a in lipid metabolism and adipocyte lipolysis. IUBMB Life 2004; 56: 379-85.

50. Imran KM, Yoon D, Lee TJ, Kim YS: Medicarpin induces lipolysis via activation of Protein Kinase A in brown adipocytes. BMB Rep 2018; 51: 249-54.

51. Saul VV, Schmitz ML: Posttranslational modifications regulate HIPK2, a driver of proliferative diseases. J Mol Med 2013; 91: 1051-58.

52. Gatti V, Ferrara M, Virdia I, Matteoni S, Monteonofrio L, di Martino S, et al: An Alternative Splice Variant of HIPK2 with Intron Retention Contributes to Cytokinesis. Cells 2020; 9: 484.

53. Yun JH, Koo JE, Koh YS: Mitogen-activated protein kinases are involved in tumor necrosis factor alpha production in macrophages infected with Orientia tsutsugamushi. Microbiol Immunol 2009; 53: 349-55.

54. Vyas S, Faucon Biguet N, Mallet J. Transcriptional and post-transcriptional regulation of tyrosine hydroxylase gene by protein kinase C. EMBO J 1990; 9: 3707-12.

55. Alarcon-Vargas D, Ronai Z: c-Jun-NH2 kinase (JNK) contributes to the regulation of c-Myc protein stability. J Biol Chem 2004; 279: 5008-16.

56. Cao Z, Umek RM, McKnight SL: Regulated expression of three C/EBP isoforms during adipose conversion of 3T3-L1 cells. Genes Dev 1991; 5: 1538-52.

57. Tettweiler G, Blaquiere JA, Wray NB, Verheyen EM: Hipk is required for JAK/STAT activity during development and tumorigenesis. PLoS One 2019; 14: e0226856.

58. Ohtsu N, Nobuhisa I, Mochita M, Taga T: Inhibitory effects of homeodomain-interacting protein kinase 2 on the aorta-gonad-mesonephros hematopoiesis. Exp Cell Res 2007; 313: 88-7.

59. Boizard M, Le Liepvre X, Lemarchand P, Foufelle F, Ferré P, Dugail I: Obesity-related overexpression of fatty-acid synthase gene in adipose tissue involves sterol regulatory element-binding protein transcription factors. J Biol Chem 1998; 273: 29164-71.

60. Sztalryd C, Brasaemle DL: The perilipin family of lipid droplet proteins: Gatekeepers of intracellular lipolysis. Biochim Biophys Acta Mol Cell Biol Lipids 2017; 1862: 1221-32.

61. Achari AE, Jain SK: Adiponectin, a Therapeutic Target for Obesity, Diabetes, and Endothelial Dysfunction. Int J Mol Sci 2017; 18: 1321.

62. Yadav A, Kataria MA, Saini V, Yadav A: Role of leptin and adiponectin in insulin resistance. Clin Chim Acta Int J Clin Chem 2013; 417: 80-4.

63. Rajala MW, Obici S, Scherer PE, Rossetti, L: Adipose-derived resistin and gut-derived resistin-like molecule- beta selectively impair insulin action on glucose production. J Clin Investig 2003; 111, 225-30.

64. Hardie DG: AMPK: a key regulator of energy balance in the single cell and the whole organism. Int J Obes 2008; 32: S7-S12.

65. Shaw RJ, Kosmatka M, Bardeesy N, Hurley RL, Witters LA, DePinho RA, et al: The tumor suppressorLKB1 kinase directly activates AMP-activated kinase and regulates apoptosis in response to energy stress. Proc Natl Acad Sci USA 2004; 101: 3329-35.

66. Towler MC, Hardie DG: AMP-activated protein kinase in metabolic control and insulin signaling. Circ Res 2007; 100: 328-41.

67. Steinberg GR, Macaulay SL, Febbraio MA, Kemp BE: AMP-activated protein kinase-the fat controller of the energy railroad. Can J Physiol Pharmacol 2006; 84: 655-65.

68. Song Y, Li X, Liu Y, Hu Y, Yang R: Arctigenin improves lipid metabolism by regulating AMP-activated protein kinase and downstream signaling pathways. J Cell Biochem 2019; 120: 13275-88.

69. Saha AK, Ruderman NB: Malonyl-CoA and AMP-activated protein kinase: an expanding partnership. Mol Cell Biochem 2003; 253: 65-70.

Expression and function of homeodomain-interacting protein kinase-2 (HIPK-2) in white and brown adipocytes

Anil Kumar Yadav

Department of molecular medicine
Graduate School

Keimyung University

Supervised by Professor Byeong-Churl Jang

(Abstract)

Homeodomain-interacting protein kinase-2 (HIPK-2), a highly conserved serine/threonine nuclear kinase, has been recently identified as a central regulator of white adipocyte differentiation and white fat development. However, at present, the expression regulation and function of HIPK-2 in adipocytes remains unclear. In this study, how HIPK-2 expression is regulated, and its expression influences the differentiation of 3T3-L1 white and immortalized brown preadipocytes. Additionally, determined the lipolysis effects of HIPK-2 inhibition in differentiated 3T3-L1 cells.The effect and mode of action of known or newly synthesized HIPK-2 inhibitor on lipid accumulation and triglyceride (TG) content during the differentiation

of 3T3-L1 white and brown preadipocytes were also assessed. Strikingly, HIPK-2 expression was highly induced in a time-dependent manner during the differentiation of both 3T3-L1 white and brown preadipocytes. Of interest, results of the pharmacological inhibition study demonstrated crucial roles of p38 MAPK, PKC, and PI3K/PKB in HIPK-2 overexpression during the differentiation of both 3T3-L1 white and brown preadipocytes.

Importantly, knockdown of HIPK-2 caused less lipid accumulation and TG content with no cytotoxicity during 3T3-L1 preadipocyte differentiation. Moreover, knockdown of HIPK-2 led to a decrease in not only expression of CCAAT/enhancer-binding protein-α (C/EBP-α), peroxisome proliferator-activated receptor-γ (PPAR-γ), fatty acid synthase (FAS), perilipin A, and adipokines such as adiponectin, leptin, and resistin but also phosphorylation of signal transducer and activator of transcription-3 (STAT-3) during 3T3-L1 preadipocyte differentiation. Furthermore, pharmacological inhibition of HIPK-2 by CX-4945, a known HIPK-2 inhibitor, greatly down-regulated not only

lipid accumulation and triglyceride (TG) content but also C/EBP-α, PPAR-ɣ, FAS, acetyl-CoA carboxylase (ACC), and perilipin A during 3T3-L1 preadipocyte differentiation. CX-4945 also increased phosphorylation of cAMP-activated protein kinase (AMPK) and liver kinase-B1 (LKB-1), an upstream activator of AMPK, while decreased intracellular ATP content during 3T3-L1 preadipocyte differentiation. CX-4945 also stimulated glycerol release and phosphorylation of hormone-sensitive lipase (HSL) and extracellular signal-regulated kinase 1/2 (ERK-1/2). Of note, treatment with PD98059, an inhibitor of ERK-1/2, attenuated CX4945-induced glycerol release and HSL phosphorylation in differentiated 3T3-L1 white adipocytes, pointing out the ERK-1/2-dependent induction of lipolysis by CX-4945. CX-4945 also could greatly reduce lipid accumulation and TG content during brown preadipocyte differentiation. Strikingly, some of the novel HIPK-2 inhibitors including KMU-011401 also had the ability to strongly reduce lipid accumulation and TG content during the differentiation of both 3T3-L1 white and brown preadipocytes. These

results collectively demonstrate that HIPK-2 expression is highly increased in a p38 MAPK, PKC, and PI3K/PKB-dependent manner and the increased HIPK-2 plays a crucial role in not only lipid accumulation and storage during the differentiation of both 3T3-L1 white and brown preadipocytes but also lipolysis in differentiated 3T3-L1 cells. These results advocate HIPK-2 and its inhibitor as a potential target and drug against obesity.

백색 및 갈색 지방세포에서 homeodomain-interacting protein kinase-2 (HIPK-2)의 발현 및 기능

아닐 쿠말 야다브
계명대학교 대학원
분자 의학과
지도교수 장 병 철

(초록)

최근의 연구에서 homeodomain-interacting protein kinase-2 (HIPK-2)가 백색 지방세포 분화 및 지방조직 발달에 관여한다는 것이 보고되었다. 그러나 현재 백색 및 갈색 지방세포 분화 과정에서 HIPK-2의 발현 기전과 기능은 불분명하다. 이에 본 연구에서 1) 백색 및 갈색 지방전구세포의 분화 과정에서 HIPK-2 발현 조절 단백질 분석 및 HIPK-2 기능을 분석하고, 2) 분화된 백색 지방세포의 지방분해에서 HIPK-2 기능을 확인하고, 3) 기존 또는 신규 합성 HIPK-2 저해제의 백색 및 갈색 지방전구세포 분화 제어 효과 및 기전을 규명하고자 하였다. 본 연구에서 3T3-L1 백색 지방전구세포 및 갈색 지방전구세포 분화 (특히, D5 (중기) 및 D8 (말기)) 단계에서 HIPK-2 과발현이 관찰되었고, 이러한 HIPK-2 과발현이 p38 MAPK 및 PKC 활성과 깊은 관련이 있음을 확인하였다. Control shRNA transfection시킨 3T3-L1 백색 지방전구세포와 비교하여, HIPK-2 shRNA

transfection시킨 세포에서 지방축적 및 중성지방 함량 감소, C/EBP-α, PPAR-ɣ, FAS, perilipin A 발현 감소 및 STAT-3 인산화 억제가 나타났다. 추가로 대조군 (용매 DMSO 투여시킨 3T3-L1 백색 지방전구세포)와 비교하여, 기존 HIPK-2 저해제 CX-4945 투여시킨 세포내 지방축적 및 중성지방 함량 감소, C/EBP-α, PPAR-ɣ, FAS, perilipin A 발현 감소, STAT-3 인산화 억제, AMPK 및 LKB-1 인산화 증가 및 ATP 함량 감소가 나타났다. 또한 분화된 3T3-L1 백색 지방세포에 CX-4945 투여 시 세포외 glycerol 방출 증가와 세포내 HSL 및 ERK-1/2 인산화가 증가되었다. 그러나 ERK-1/2 저해제 PD98059 투여 시 분화된 3T3-L1 백색 지방세포에서 CX-4945에 의한 지방분해 (glycerol 방출 및 HSL 인산화 증가)가 크게 약화되었다. 이들 결과는 CX-4945가 지방분해 효과를 가지며 이것이 ERK-1/2 의존적임을 말해주었다. 추가적으로 본 연구를 통해 신규 의약합성된 HIPK-2 저해제 KMU-011401 투여 시 분화유도제에 의한 3T3-L1 백색 지방전구세포 및 갈색 지방전구세포내 지방축적 및 중성지방 함량 증가가 크게 감소되었다. 상기 실험결과를 종합해 볼 때 백색 및 갈색 지방전구세포 분화 과정에서 일어나는 p38 MAPK 및 PKC 의존적 발현 증가된 HIPK-2는 C/EBP-α, PPAR-ɣ, FAS, perilipin A 발현 증가 및 STAT-3 활성화를 통해 이들 지방세포내

지방축적 및 지방저장에 중요한 기능을 수행하는 것으로 보인다. 이들 결과는 HIPK-2/HIPK-2 저해제가 향후 비만의 예방 및 치료의 잠재적 표적 분자/치료제로서활용(개발)될 가능성을 제시한다.